OBSTETRICS

Visualization of microbes by 16S in situ hybridization in term and preterm placentas without intraamniotic infection

Maxim D. Seferovic, PhD; Ryan M. Pace, PhD; Matthew Carroll, MD; Benjamin Belfort; Angela M. Major; Derrick M. Chu, PhD; Diana A. Racusin, MD; Eumenia C. C. Castro, MD, PhD; Kenneth L. Muldrew, MD, MPH; James Versalovic, MD, PhD; Kjersti M. Aagaard, MD, PhD

BACKGROUND: Numerous reports have documented bacteria in the placental membranes and basal plate decidua in the absence of immunopathology using histologic techniques. Similarly, independent metagenomic characterizations have identified an altered taxonomic makeup in association with spontaneous preterm birth. Here we sought to corroborate these findings by localizing presumptive intact bacteria using molecular histology within the placental microanatomy.

OBJECTIVE: Here we examined for microbes in term and preterm gestations using a signal-amplified 16S universal in situ hybridization probe set for bacterial rRNA, alongside traditional histologic methods of Warthin—Starry and Gram stains, as well as clinical culture methodologies. We further sought to differentiate accompanying 16S gene sequencing taxonomic profiles from germ-free (gnotobiotic) mouse and extraction and amplicon contamination controls.

STUDY DESIGN: Placentas were collected from a total of 53 subjects, composed of term labored (n = 4) and unlabored cesarean deliveries (n = 22) and preterm vaginal (n = 18) and cesarean deliveries (n = 8); a placenta from a single subject with clinical and histologic evident chorioamnionitis was employed as a positive control (n = 1). The preterm cohort included spontaneous preterm birth with (n = 6) and without (n = 10) preterm premature rupture of membranes, as well as medically indicated preterm births (n = 10). Placental microbes were visualized using an in situ hybridization probe set designed against highly conserved regions of the bacterial 16S ribosome, which produces an amplified stable signal using branched DNA probes. Extracted bacterial nucleic acids from these same samples were subjected to 16S rRNA metagenomic sequencing (Illumina, V4) for course taxonomic analysis, alongside environmental and kit contaminant controls. A subset of unlabored, cesarean-delivered term pregnancies were also assessed with clinical culture for readily cultivatable pathogenic microbes.

RESULTS: Molecular in situ hybridization of bacterial rRNA enabled visualization and localization of low-abundance microbes after systematic high-power scanning. Despite the absence of clinical or histologic chorioamnionitis in 52 of 53 subjects, instances of 16S rRNA signal were confidently observed in 13 of 16 spontaneous preterm birth placentas, which was not significantly different from term unlabored cesarean specimens (18 of 22; $P > .05$). 16S rRNA signal was largely localized to the villous parenchyma and/or syncytiotrophoblast, and less commonly the chorion and the maternal intervillous space. In all term and unlabored cesarean deliveries, visualization of evident placental microbes by in situ hybridization occurred in the absence of clinical or histologic detection using conventional clinical cultivation, hematoxylin—eosin, and Gram staining. In 1 subject, appreciable villous bacteria localized to an infarction, where 16S microbial detection was confirmed by Warthin—Starry stain. In all instances, parallel sample principle coordinate analysis using Bray-Cutis distances of 16S rRNA gene sequencing data demonstrated consistent taxonomic distinction from all negative or potential contamination controls ($P = .024$, PERMANOVA). Classification from contaminant filtered data identified a distinct taxonomic makeup among term and preterm cohorts when compared with contaminant controls (false discovery rate <0.05).

CONCLUSION: Presumptively intact placental microbes are visualized as low-abundance, low-biomass and sparse populations within the placenta regardless of gestational age and mode of delivery. Their taxonomic makeup is distinct from contamination controls. These findings further support several previously published findings, including our own, which have used metagenomics to characterize low-abundance and low-biomass microbial communities in the placenta.

Key words: Human microbiome, in situ hybridization, placenta, placental bacteria, placental microbes, placental microbiome, PPROM, preterm birth, preterm labor

Despite decades of research and incremental progress, preterm birth (PTB) persists as a primary contributor to perinatal morbidity and mortality. PTB is the single greatest risk factor for poor long-term health outcomes among children, including chronic lung disease, neurologic impairment, and cerebral palsy.[1] Studies in animal models have implicated that inflammation and infection results in early onset of labor,[2–6] while human studies have suggested that fetal-placental inflammatory mechanisms are key factors in the initiation of at least a subset of spontaneous PTB (sPTB).[7–13] Fetal-placental inflammation has similarly been implicated in the spontaneous onset of labor.[10–14] However, the true association of placental, chorion-amnion, or intraamniotic microbes with inflammation remains unclear,[15,16] as the presence of microbiota have been detected with term births, and microbes (particularly commensals) are not necessarily accompanied by histologic or molecular markers of inflammation. In this study, we hypothesized that with diligent use of microscopy we would be able to detect and

Cite this article as: Seferovic MD, Pace RM, Carroll M, et al. Visualization of microbes by 16S in situ hybridization in term and preterm placentas without intraamniotic infection. Am J Obstet Gynecol 2019;221:146.e1-23.

0002-9378/$36.00

https://doi.org/10.1016/j.ajog.2019.04.036

Click Supplemental Materials under article title in Contents at ajog.org

AJOG at a Glance

Why was this study conducted?

To identify and localize bacteria within the placental microanatomy in term and preterm pregnancies.

Key findings

Sparse, very low-biomass bacteria were observed by histological and 16S rRNA gene sequencing methods regardless of gestational age.

What does this add to what is known?

The findings corroborate previous histological, culture based, and metagenomic studies that identified sparse bacteria in the placenta.

visualize even rare and low-abundance placental microbes in the absence of intraamniotic infection. We further hypothesized that utilization of an in situ hybridization (ISH) probe set for the bacterial 16S ribosome (16S rRNA) producing an amplified stable signal with branched DNA probes sets would enable us to predictably localize their presence within the placental microarchitecture, even as a low biomass and sparse community.

There is a potential discordance between the absolute presence or absence of bacteria n the intraamniotic environment and the occurrence of PTB.[8,14,16–23] Mounting evidence suggests that the intrauterine environment contains bacteria of yet unknown significance, and a large number of independent research groups have repeatedly reported on the detection of bacteria in both the presence and absence of inflammation or clinically evident infection.[10,16–55] Although there is a significant correlation between the presence of positive bacterial cultures and the occurrence of sPTB, there is similarly substantial historical and recent evidence that the presence of bacteria per se is not sufficient to trigger the early onset of labor in human populations.[10,16–39,46–55] For example, observational studies suggest that placental specimens without histologic or clinical evidence of inflammation harbor bacteria,[17] and live bacteria are recoverable by culture from greater than half of term or near-term (>34 week) placentas.[16] Similarly, others have reported the capacity to cultivate a diverse bacterial population from the placental parenchyma in 25% of maternally indicated preterm deliveries[25,40] or from fetal cord blood.[41] More recently, metagenomic sequencing technologies have provided genomic-based evidence for a unique collective community of bacteria contained within both term and preterm placentas.[27–31;42–55] Collado et al[27] have reported not only shared microbiota between the placenta and the neonatal meconium, but the presence of viable organisms including *Propionibacterium* and *Staphylococcus* from the placenta and amniotic fluid at the time of cesarean delivery in a cohort of full-term pregnancies. Shifts in the taxonomic makeup of these communities, rather than the absolute presence or absence of a single bacterial taxa, are associated with a remote history of maternal antenatal infection, excess gestational weight gain, preeclampsia, and sPTB.[28,29,39,42–44,46–55]

However, metagenomic and 16S-based sequencing characterizations are also subject to several limitations. First, it has been assumed that short-read sequencing may not differentiate intact bacteria from what may be remnant nucleic acid of phagocytosed organisms. Second, in the absence of precise microdissection techniques with targeted sequencing, metagenomics does not enable accurate localization of the bacteria within the microanatomy of the heterogeneous placenta. Finally, concern for interpretation of 16S-based metagenomic sequencing data from low-abundance samples has recently been raised[47] and suggested to be influenced by low-level microbial DNA contained within kit reagents.[56–59]

To address these limitations, in the current study we utilized state-of-the-science branched DNA signal-amplified fluorescence microscopy in an effort to localize placental bacterial rRNA, making comparisons to conventional staining and standard clinical cultivation techniques. We secondarily expanded our analysis to a cohort of term, unlabored cesarean-delivered placentas in the absence of any evidence of infection. Finally, we performed 16S-based metagenomic sequencing with the appropriate V4 primers to compare the taxonomic composition of the placental microbes against kit-negative and germ-free (GF) gnotobiotic mouse placental controls. Our approaches were complementary: 16S rRNA ISH with stable signal amplification allowed us to visualize, roughly quantify, and localize the placental microbiota and their transcribed RNA, while 16S gene amplification and sequencing of V4 targets provided parallel relative abundance estimates pertaining to which placental taxa were present.

Collectively, our findings reported herein document sparse but reproducible 16S rRNA fluorescent labeling, being visualized in the villus and chorion at low but observable abundance in both labored and unlabored term births and PTBs. Using appropriate methodology and controls, we could also demonstrate that parallel specimens harbored metagenomes that were distinct from potential environmental contaminants. This report serves as histologic molecular evidence of microbes in the placental villous tissue, and further supports consistent and numerous reports that have used histologic, culture-based, and metagenomic approaches to document low-abundant, low-biomass placental microbes in the term and preterm human placenta.

Materials and Methods

Sample collection, tissue dissection, microbial culture/cultivation, and histology

Sample collection

Placental collections were performed among enrolled subjects with informed consent and the approval of the Baylor

College of Medicine Institutional Review Board (H-34056, H-26364, and H-27393) at the time of admission to the labor and delivery unit. In response to reviewer requests, ultimately 2 cohorts were collected. The initial subject cohort was composed of more preterm than term births, with a mix of vaginal and cesarean deliveries. Following initial review of our study, the reviewers and editors suggested that we additionally perform placental collection, microscopy, 16S sequencing, and clinical cultivation studies of a second cohort of 29 subjects composed largely of term, unlabored, and cesarean births. Patient characteristics were assessed by ANOVA or Fisher exact test where appropriate. Statistics were performed using Prism software (GraphPad v6.01, La Jolla, CA). Statistical significance was determined at $P < .05$.

For the first cohort, inclusion criteria included all preterm and term pregnancies not meeting exclusion criteria (eg, clinical chorioamnionitis, multiple gestations, placental abruption, and placenta previa). For the second cohort, we included largely term pregnancies that were cesarean delivered and unlabored, which met the same exclusion criteria as the initial cohort (eg, clinical chorioamnionitis, multiple gestations, placental abruption, and placenta previa). In addition to sequencing and histologic analysis of this second cohort, diligent clinical cultivation of placental tissue, cord blood, and environmental controls was performed in our clinical microbiology laboratory and included reference-standard aerobic and anaerobic clinical cultivation protocols. As a positive control reference, a single pathology-proven chorioamnionitis placenta and archived lung specimens (described below) were used for control comparisons.

Dissection of placental tissue

Dissection of placental tissue was carried out as previously described.[29] Briefly, immediately following delivery placentas were removed to a clean, chemical- and ultraviolet-sterilized, class II B2 biosafety cabinet in a sterile container, and dissections carried out using sterile disposable surgical instruments on certified DNA- and RNA-free cell culture–grade containers. No containers or instruments were reused with any collection or dissection. Membranes were removed from the fetal side with a sterile scalpel and forceps. New sterile disposable scalpel and forceps were then used to extract a small core of tissue, with great care taken to avoid contamination by the placental surface. In an abutting area of the placenta, a full placental cross section was dissected from the fetal-to-maternal side using another new and sterile set of disposable surgical instruments. Samples were then placed in an autoclaved and sterile container for fixation in 10% neutral buffered formalin (Fisher Scientific, Pittsburgh, PA) overnight (and a period not ever exceeding 24 hours). All tissue preparation and fixation from this point forward was carried out by a clinical pathology–trained histologist with decades of experience with fluorescence in situ hybridization (FISH) and over 13 years of quality-assured experience with the Therapeutic Microbiology Lab of Texas Children's Hospital. Sterile fixed sections were then mounted in cassettes under similarly sterile conditions, and automated paraffin embedding was done in a dedicated research laboratory space, which is spatially distinct from the clinical laboratory and uses exclusively a research-dedicated processor (Tissue-Tek VIP, Sakura Finetek USA, Torrance, CA), embedder, and microtome to control for contamination. The processed placental tissue was housed in a retort, and reagents were vacuumed into the retort. Once the tissue processing was complete, tissue was embedded employing fresh sterile paraffin and autoclaved forceps. Thin 4-μm sections were then cut from blocks using a microtome with a clean-sterile fresh blade (Leica) for each specimen, with the first 10 sections being discarded to remove externally exposed specimen areas and alternately access unexposed inner tissue/block to minimize risk of external microbial contamination. Serial sections were then placed onto positively charged adhesive slides for subsequent staining and probing. Dissected placental core sections were sent for DNA extraction (PowerSoil, Qiagen, Venlo, the Netherlands) and V4 16S rRNA gene sequencing.

Clinical culture/cultivation

For the second cohort only, an additional sterilely dissected placental core sample, cord blood, and environmental contamination controls were sent for clinical culture in an independent and blinded fashion to the CLIA-certified Clinical Microbiology Laboratory at Ben Taub Hospital, Harris Health System (Houston, TX). Environmental swab cultures were performed on any possible sources of contamination, which included the inside and outside of the placental container, the handles used for transport from the delivery or operative room to the designated clean-sterile research dissection hood, and the dissection surface. Clinical culture swabs were placed in a sterile specimen container and transported immediately to the clinical microbiology laboratory. With the exception of A-7 Mycoplasma/Ureaplasma media (Remel, Inc, San Diego, CA), all other media were obtained commercially from Becton Dickinson (Franklin Lakes, NJ).

Swab samples were placed in thioglycolate broth and agitated and then the liquid was plated to solid media. Tissue samples were homogenized in thioglycolate broth and then plated to solid media. Samples were plated on 5% sheep blood and MacConkey agars, incubated for 3 days at 35°C in ambient air, and examined daily for growth. Samples were also plated on chocolate agar, incubated for 3 days at 35°C in 5% CO2, and examined daily for growth. Culture in thioglycolate broth was performed by incubating at 35°C in ambient air for 3 days and examining daily for growth. Anaerobic culture of samples was performed by plating to brucella agar, phenyl ethyl alcohol agar, and kanamycin/vancomycin agar media. These plates were incubated in anaerobic conditions at 35°C for 5 days and examined daily for growth. Culture for *Mycoplasma* and *Ureaplasma* species was performed by plating samples on A-7 Mycoplasma/Ureaplasma agar, incubating for 14 days at 35°C in ambient air, and examining daily for growth.

Both venous and arterial cord blood was sampled using a sterile needle and syringe, following circumferential alcohol swabbing of the cord, into a sterile BACTEC Peds Plus/F Culture Vial (Becton Dickinson, Sparks, MD), per manufacturer's instructions. If positive for growth, fluid extracted from the vial would then be subcultured on the plate media described above for further identification.

All isolates were identified by Matrix-Assisted Laser Desorption/Ionization Time-of-Flight mass spectrometry using the Bruker MALDI Biotyper (Becton Dickinson).

Histology

Staining with 3 different standard methods (hematoxylin–eosin [H&E], Gram, and Warthin–Starry [WS] stains) was uniformly performed in the clinical Anatomical Pathology Laboratory of Texas Children's Hospital (Houston, TX). Each of these 3 stains detects microbes differently and, like all stains, provides contrast to improve feature identification with limited specificity. Taylor's Brown–Brenn Modified Gram stain, which is used for the detection and differentiation of gram-positive and gram-negative bacteria,[60] is dependent on dyes becoming trapped within membranous structures. Crystal violet is first applied and precipitated, while peptidoglycan structures preferentially retain the precipitate, with safranin dye then applied as a counterstain. WS uses silver stain to introduce contrast; it also has a long history of clinical use for detection of spirochetes, among other taxa.[61] Staining and development was automated, using an Artisan Link Pro Automatic special stainer (Dako, Glostrup Denmark).

16S ribosome RNA in situ hybridization

A first-pass attempt at labeling the 16S rRNA was carried out using FISH, employing the well-described generic 16S rRNA-specific probe (EUB338) following a standard FISH protocol (GCTGCCTCCCGTAGGAGT-Cy3; Integrated DNA Technologies, Coralville, IA), and a scramble control. Because the placenta has abundant autofluorescent structures including collagenous matrices, omnipresent trophoblast cells, and erythrocytes, rendering detection of fluorescent FISH probes (such as EUB338) in the placenta is very challenging.[62–64] Reliably identifying true 16S rRNA fluorescent signal from background was also particularly challenging because of the nonubiquitous, rare, and focal nature of microbial signal in tissue, and also in part owinge to their small size relative to surrounding structures (<1/1000 volume of a nucleus, which is near the limits of light microscopy resolution). Furthermore, we found that the fluorophore signal from the EUB338 probe was quenched with the prolonged and extensive high-power manual scanning under illumination, which was required for the detection of these sparse findings with this standard approach.

Given the challenges in resolving to high confidence even known instances of cultivation-positive chorioamnionitis placental specimens by FISH with the EUB338 probe, we sought alternative methodologies of ISH. To achieve the goal of distinguishing low-abundance microbes reliably and confidently from placental background, we sought stable and specific 16S rRNA probes that also avoided quenching and enabled reliable bacterial localization in the microarchitecture of the placenta. We thus compared EUB338-labeled specimens with those labeled using alternative fluorescent probes. Specifically, we found that the ViewRNA ISH Tissue 1-Plex Assay (ViewRNA, Affymetrix, Santa Clara, CA) had the advantage of employing a stable chromogen that could be scanned for long periods of time both in bright field (without background autofluorescence) and in fluorescence, and rendering higher signal intensity via amplification that was several orders of magnitude increased. The ViewRNA ISH signal is based on specific amplification of target RNA probes (ie, 16S rRNA) that is dependent on 2 paired, sequence-specific, separate adjacent probes to hybridize on a transcript, facilitating significantly greater specificity over conventional FISH. The assay provides sensitive and robust in situ detection within formalin-fixed paraffin-embedded tissue sections with a single-copy sensitivity, as originally described.[65]

The probing and tissue preparation was performed as per manufacturer's instruction (ViewRNA ISH Tissue 1-Plex, Affymetrix). First-iteration experiments with placental specimens used Conroy's as fixative, which is typically employed with the goal of preserving the mucous lining for histologic bacterial studies (including classical 16S FISH) in intestinal lumen specimens. However, Conroy's fixative did not adequately preserve the placental tissue architecture in our hands. In the absence of a need to preserve mucus, and leveraging the expertise of our histopathology investigators, we thereafter fixed placental specimens in formalin and optimized antigen retrieval methods to recover the signal from cross-linked, formalin-fixed tissue. In an effort to minimize risk of environmental contamination, all experiments were carried out using the single-day option. Briefly, slides were first baked at 60°C, then deparaffinized with fresh sterile clean xylene and ethanol; then a heat pretreatment was carried out at 95°C, followed by a sterile clean protease digestion optimized to 10 and 20 minutes, respectively. Samples were then probed in uniform and systematic sequence: first for RNA hybridization, then an adapter probe, an amplification probe, and finally an enzyme-labeled probe. All hybridizations were at 40°C using a programmable hybridizer (ThermoBrite, Leica, Wetzlar, Germany), and interspersed with washing steps in provided clean wash buffer, diluted with Milli-Q water, then refiltered. Hybridization times were as per manufacturer's instructions (3 hours, 40 minutes, 15 minutes, 40 minutes, and 15 minutes, respectively). The 16S rRNA-specific hybridization probe set consisted of 6 distinct probes (CACGAGCTGACGACAACCATGC, CACGAGCTGACGACAGCCATGC, CGGGACTTAACCCAACACTTCACG, CGGGACTTAACCCAACATCTCACG, CGGGAC

TTAACCCAACATTTCACG, GGGAC TTAACCCAACACCTCACG) that were designed against highly conserved regions of bacterial 16S rRNA sequence (Affymetrix). NCBI Blast searches against both the human genome and transcriptome reveal no significant oligonucleotide identity or sequential cross-hybridization (expected value >5.5, coverage <72%), thus virtually eliminating the possibility that fluorescence hybridization labeling could represent human DNA/RNA nonspecific hybridization rather than 16S bacterial rRNA labeling. Moreover, the sequential hybridizations layer sequence-matched DNA probes coupling 16S rRNA probes to multiple labeled probes conjugated to alkaline phosphatase enzymes. Thus, a single ribosomal hybridization would conjugate more than 1 alkaline phosphatase, yielding significant and impressive fluorescent signal amplification when compared with conventional FISH with the EUB338 probe. Finally, the fluorescent-labeled slides were developed with provided Fast Red reagent substrate for 20 minutes at 40°C, which, catalyzed by alkaline phosphate, produces a chromogen that is visible in both bright field and fluorescence. To provide cellular and subcellular context to map architectural features, the probed slides were counterstained with both a very light hematoxylin and 4′,6-diamidino-2-phenylindole (DAPI; Sigma-Aldrich, St. Louis, MO) stains, and mounted with Faramount aqueous medium (Dako).

Histologic analysis

H&E and Gram-stained specimens were first evaluated in a blinded fashion by a perinatal pathologist with accepted and recognized expertise in placental histology to assess for inflammation (E.C.). ISH-labeled slides of serial sections probed for 16S rRNA were subsequently examined using an Eclipse 90i fluorescent microscope (Nikon Instruments, Melville, NY) with a 10× eyepiece. (Henceforth, where magnification is labeled or referred to in the text, it is referring to the objective magnification only.) Manual scanning of the slides was made under bright-field illumination at 60× or 100× (high power), moving systematically field-to-field across the tissue in intersecting grids (X to X, then Y to Y planes). As a first pass for ultimately time-consuming analyses in the Z plane under high power, systematic attempts were made to automate the capturing of sequential confocal Z-stacks with stitched images of uniform 1 × 1-cm blocks. This systematic approach should have produced a 3-dimensional image that could then be theoretically subjected to automated analysis. However, in our hands, given the high power and resolution required to reliably detect submicron bacterial rRNA, and the size of field required, the number of stitched images readily exceeded the microscope primary memory. We thus abandoned such an automated approach in favor of more tedious but ultimately reliable manual scanning, systematically shifting fields and adjusting focus through the Z planes. Tissues were sequentially examined until either at least 3 cellular or subcellular features were identified or all tissue on the slide had been examined. Uniform alterations between fluorescent and bright-field channels were used extensively for image capture and to confirm presumptive true signal from likely or probable artifact. Fluorescent images of DAPI for nuclei and naïve FITC for the tissue (background fluorescence) were taken using autoexposure conditions, while TRITC (16S rRNA probe signal) were taken with a consistent exposure calibrated from the positive (cultivation-confirmed) chorioamnionitis control. Bacterial density was estimated in a subset that was systematically and exhaustively examined, based on an inferred volume calculated from the mounted tissue dimensions estimated at 1.5 × 1.5-cm sections of 4 μm thickness. Images captured are unmodified except for cropping and labeling. For the second unlabored term cohort, scale bars are included in response to reviewers. For legibility and esthetics, the original Nikon Elements—produced scale bars are covered and reproduced with standardized uniform bars of the same accurate scale (Figure 5 in Results).

DNA extraction for 16S rRNA gene sequencing

Samples were extracted and subjected to V4 16S rRNA gene sequencing and analysis under stringent clean and sterile techniques, as previously described.[29] The 2 cohorts were extracted separately using the same personnel, reagents, and methodology but run on the same massively parallel sequencing runs (Illumina MiSeq, San Diego, CA). Because 2 cohorts were ultimately necessitated by reviewer and editor request (as discussed above), the first cohort of largely preterm subjects was therefore sequenced twice to allow for side-by-side comparison and minimize any potential batch bias. Approximately 150 mg of placental sample was collected and extracted using Power Soil DNA isolation kit (MoBio, Carlsbad, CA). Gnotobiotic GF mouse placenta (n = 4) and "kit-negative" extractions (n = 6) were processed and sequenced in parallel as contamination controls. In all studies, "kit-negative" refers to Power Soil DNA extractions without placental tissue, which were in all extraction, amplification, and sequencing steps performed in direct parallel manner (ie, having been performed side-by-side with placental specimens at the same time, space, and exposure, with identical reagents, equipment, and personnel). GF mouse placentas were collected from 3 timed pregnant mice on day 18.5 by sterile cesarean delivery and dissected under the same sterile conditions as human placentas for extraction but included a full one quarter of a mouse placenta (approximately 40 mg) in each case. As with placentas, dissection was carried out using a biosafety containment hood that was chemically and ultraviolet sterilized, and dissection was done on sterile RNA-free cell culture—grade plastics with a sterile surgical scalpel. The extracted DNA was subjected to V4 amplification of the 16S gene region using barcoded Illumina adapter-containing primers 515F and 806R51 and sequenced with the 2 × 250-

bp cartridges on the MiSeq platform (Illumina).

16S rRNA gene sequencing and data processing

Samples were submitted for Illumina MiSeq sequencing (2 × 250 bp) of the 16S rRNA gene (V4 hypervariable region) at the Center for Microbiome and Metagenomic Research at Baylor College of Medicine. The following primers were used: forward primer, 5′-GTGCCAGC MGCCGCGGTAA-3′; reverse primer, 5′-GGACTACHVGGGTWTCTAAT3′. Raw reads were demultiplexed using idemp (https://github.com/yhwu/idemp). The demultiplexed data then had primers/adapters removed with cutadapt[66] and were further quality filtered and split into paired and unmatched reads with Trimmomatic.[67] Quality-filtered data were then imported and processed with DADA2 (v1.6)[68] in R (v3.4.3) (https://www.r-project.org/). Briefly, sequences were manually examined for drop-off in sequencing quality and subsequently the forward and reverse reads were quality filtered and uniformly trimmed using the filterAndTrim() command. Error rates for both the forward and reverse reads were learned using the default settings. Sequence variants were inferred after sequence dereplication and paired reads merged to generate the amplicon sequence variants (ASVs). ASVs longer or shorter than the expected amplicon size were filtered out. Chimeric ASVs were identified using the command removeBimeraDenovo() using the consensus method. ASVs were assigned taxonomy with the assignTaxonomy() function using RDP's naïve Bayesian classifier against the provided Silva reference/training database (silva_nr_v128_train_set.fa.gz), with species-level assignments also made using the addSpecies() function against the provided Silva species training data (silva_species_assignment_v128.fa.gz). The final ASV tables containing the abundance of each ASV in every sample were then imported into the phyloseq (v1.23.1)[69] R package for downstream analysis. ASV tables were then filtered to remove nonbacterial ASVs, including mitochondria and chloroplast, and unclassified bacterial ASVs, as well as to remove samples with subsequent zero ASV counts. Samples were rarefied to 75% of the minimum sample reads for multidimensional scaling and alpha diversity analyses using the phyloseq rarefy_even_depth() function. PICRUSt2 was used to infer predicted functional pathways by placing ASV sequences into the PICRUSt2 reference phylogeny, followed by the mp method for hidden-state prediction. The PICRUSt2 predicted pathway abundances (nonstratified) were then analyzed.[70]

Prevalence-based filtering of putative contaminant amplicon sequence variants

Prevalence-based filtering of putative contaminant ASVs was performed using the R package decontam (v0.99.1).[71,72] DNA extraction blanks contemporaneously generated and processed in parallel with biological samples (n = 6) were used as negative controls in the filtering procedure. ASV tables were used as the input for both the isContaminant() function and the recommended function for filtering contaminants from low microbial biomass samples, isNotContaminant(). For both isContaminant and isNotContaminant the default parameters were employed (method = "prevalence," threshold = 0.5, normalize = TRUE, detailed = TRUE). DNA extraction blank controls and ASVs lacking statistical support (putative contaminants) based on the isNotContaminant results were then filtered from the ASV table for downstream analysis.

Statistical analyses

Except where noted, all statistical analyses were performed using R (version 3.4.3) and/or GraphPad Prism (GraphPad Software Inc, La Jolla, CA). The R packages vegan (v2.5-2),[73] phyloseq (v1.23.1),[69] and ggplot2 (v3.0.0)[74] were used to perform and visualize cluster analyses and ordinations.

Data availability

The 16S targeted amplicon sequence data generated from this analysis have been deposited in the Sequence Read Archive under bioproject ID PRJNA511648.

Results

16S rRNA in situ hybridization for in situ visualization and localization of placental microbes in the villous tree

Signal-amplified probe sets specific for bacterial 16S ribosomal RNA were first tested against known infected lung and placental tissue (clinical and histopathology-confirmed pneumonia and chorioamnionitis) to validate probe set specificity and estimate resolution. Gram staining showed both rods and cocci of archived infected lung tissue (subjects with pneumonia) utilized as a positive control (Figure 1, Ai). Fluorescent imaging of the same tissue showed signal emanated from bacteria in probed infected tissue (Figure 1, Aiii) but not in probe-negative controls (Figure 1, Aii), indicating probe specificity. Placental tissue from cases of clinically confirmed chorioamnionitis had substantial fluorescent signal overlapping with the infected areas of the chorioamnion as determined by conventional H&E and Gram staining (Figure 1, B). Infection within the villus was also apparent in the same placenta, and was easily assessed both in bright field and in matching fluorescent fields (Figure 1, Ci and Cii). This was in contrast to the probe-free control, which despite having occasional background artifact features (for example, clumps of dye reagent, here indicated as likely artifact), exhibited no bright-field or fluorescence signal (Figure 1, Ciii and Civ). In all instances, we performed and display both bright-field and fluorescent images side-by-side, meeting the highest standards of rigor and assuring that artifact and autofluorescence is not confused with 16S rRNA−specific detection.

Having verified the probe set specificity and sensitivity, we next examined placentas collected from subjects with PTB and healthy term pregnancies (Figure 2). In total and inclusive of the single case of chorioamnionitis, 53 subjects' placentas were interrogated. Placentas from the largely PTB cohort were further classified as medically indicated (n = 10), spontaneous (sPTB, n = 7), or sPTB following preterm premature

FIGURE 1
Amplified 16S ribosomal RNA probes employing in situ hybridization reveal bacteria in situ in infected tissues

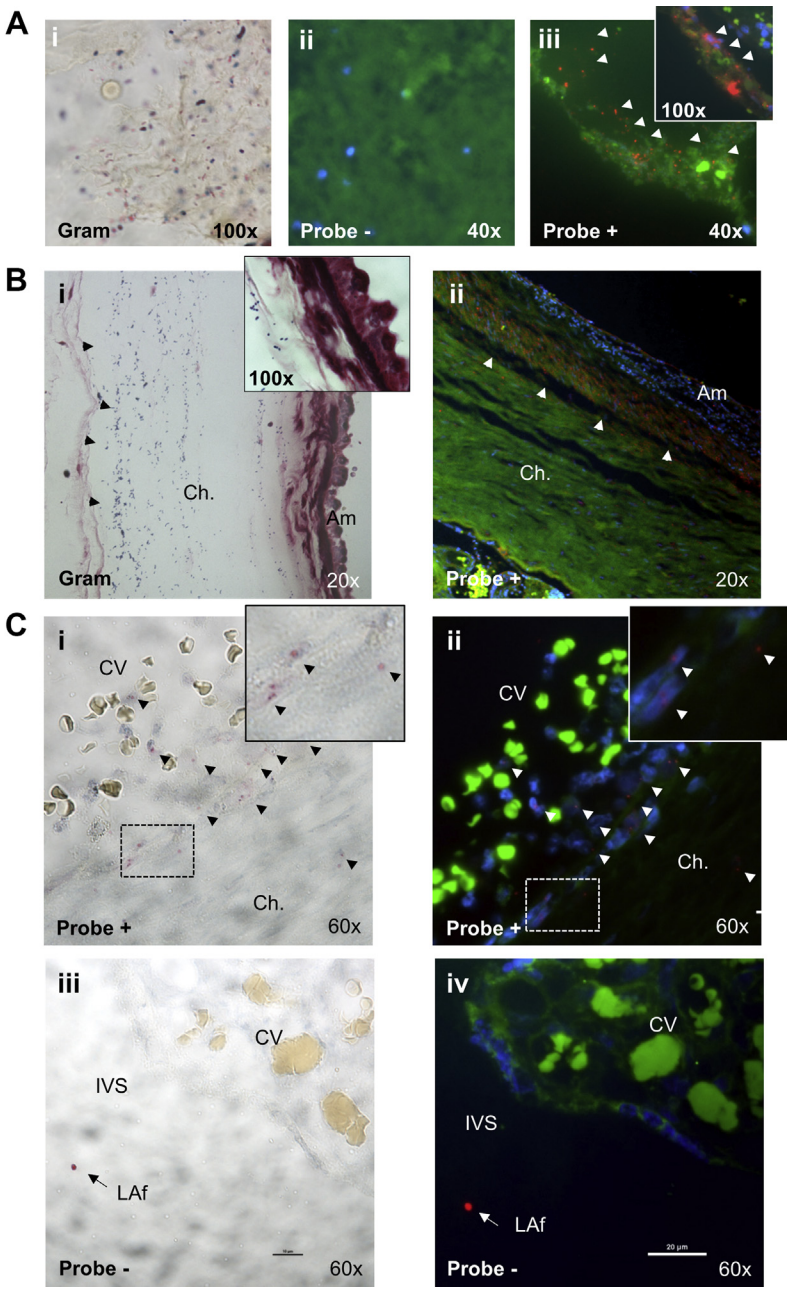

Infected archived lung and placental tissue was used to verify probe specificity and sensitivity vs a standard Gram stain. **A,** Infected archived lung tissue (pneumonia) with gram-positive and gram-negative bacteria (i) exhibited strong red fluorescence with 16S probe signal (arrows) (iii) but not with a probe-free control serial section (ii). **B,** Infected chorioamnion of placenta from a single subject, as verified by examination by Gram stain (i), exhibited corresponding fluorescence from the bacterial ribosomal probe (ii) (red, arrows). **C,** 16S signal is apparent in chorioamnion and villous tissue of infected placenta in matching bright-field (i) and fluorescent images (ii). (iii, iv) Label-free control section, depicting a typical excluded background feature.

Am, amnion; *Ch*, chorion; *CV*, chorionic villi; *LAf*, likely artifact; (red: 16S rRNA; blue: DAPI; green: autofluorescence).

Seferovic et al. Visualization of placental microbiota. Am J Obstet Gynecol 2019.

rupture of membranes (PPROM) (n = 6) (Figure 2, B); an additional 3 sPTB subjects were included in the culture/cultivation study group. The gestational age at delivery was significantly different between term and PTB cases, but comparable within the preterm cohort (mean 34.1 weeks), regardless of PPROM and spontaneous vs indicated substratification (Figure 2, B). There were no significant differences in maternal age or cesarean delivery rate between the preterm groups (Figure 2, B). Consistent with exclusion criteria, gross evidence of chorioamnionitis and villitis was not observed, and analysis of H&E and Gram stain failed to reveal abundant bacteria when viewed by a recognized and boarded perinatal pathologist (E.C.) specializing in anatomic perinatal and placental histology and molecular pathology (who was blinded to clinical characteristics, including term and preterm status). For the culture/cultivation cohort, unlabored term pregnancies that were cesarean delivered were specifically recruited in an effort to eliminate risk of vaginal contamination, with a small number of preterm births as reference controls. The placental villous tissue, as well as venous and arterial cord blood, and an environmental container and dissection surface swabs were similarly assessed by both clinical culture and histology (Figure 2, A). The cultivation studies were carried out under the supervision of a boarded clinical microbiologist (K.M.M.), who was similarly blinded to the specimens' clinical characteristics.

Following extensive trial and error with several off-the-shelf FISH methodologies (described in Methods), systematic manual examination of serial sections of placentas from term pregnancies probed by universal 16S rRNA probe sets designed with branched DNA signal amplification allowed for successful discrimination and visualization of placental microbes at high power (60−100×). Representative images are shown in Figure 3. Amplified 16S ribosomal RNA signal appears red, while the host cell nuclei stains blue with DAPI. Green signal is tissue autofluorescence,

FIGURE 2
Study design and subject characteristics

A

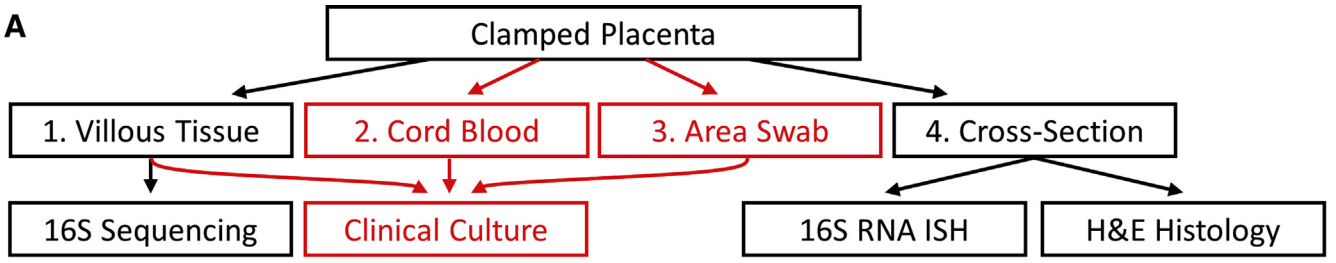

B

	Culture Study Group (*N*=26)			Preterm Study Group (*N*=27)			
	Clinical Chorio.	*sPTB*	*Term Unlabored*	*Term*	*sPTB*	*PPROM*	*iPTB*
Number of Subjects (*n*)	1	3	22	4	7	6	10
Ave Maternal Age	25.2	29.12	30.5	26.2	25.6	36.6	29.2
Pre-Gestation BMI	30.0	31.0	30.6	33.4	30.2	34.4	30.3
Hispanic (%)	100	100	91	100	100	83	90
Ave GA (weeks)	37.1	33.6	38.8	39.3	34	34.5	33.6
Augmentation (%)	100	33	0	100	43	57	80
Caesarian (%)	0	33	100	25	14	33	40
GBS positive (%)	Unknown*	0*	32*	0	28	16	10
Antenatal Infection (%)	100	100	41	25	29	16	30
Antibiotic use (%):							
1st trimester	0	0	18	0	14	0	10
2nd trimester	0	0	27	25	29	0	0
3rd trimester	100	100	0	0	57	83	50
Endometritis (%)	0	0	0	0	0	0	0
Cl. Chorioamnionitis (%)	100	0	0	0	0	0	0

Placental Histology	*Clinical Chorio.*	*sPTB*	*Term Unlabored*	*Term*	*sPTB*	*PPROM*	*iPTB*
Chorioamnionitis (%)	100	0	0	0	0	16	10
Villitus (%)	0	33	5	0	14	16	0
Deciduits (%)	0	33	9	0	14	16	10
Meconium (%)	0	0	23	50	0	0	0
Positive Gram stain (%)				0	0	0	0

Positive Microbial Culture	*Clinical Chorio.*	*sPTB*	*Term Unlabored*
Environmental Swab (%)	0	0	5
Venous cord blood (%)	0	0	0
Arterial cord blood (%)	0	0	0
Placental tissue (%)	0	0	0

sPTB: Spontaneous preterm birth, iPTB: indicated preterm birth, PPROM: Preterm premature rupture of membranes.
*5/26 subjects unknown

with fetal and maternal red blood cells appearing bright green. 16S rRNA signal is observed in the chorionic villi (Figure 3, A), as well as straddling or abutting the separating syncytiotrophoblast layer and apparently following the contour of the villous syncytiotrophoblast (Figure 3, B). Confident bacterial rRNA signal was similarly visualized lining (but not within) the maternal intervillous space (Figure 3, C). In 1 instance, a few bacteria were observed in the fetal chorionic vessels (Figure 3, D). In several instances, the lumen of the chorionic villi harbored microbiota (Figure 3, E). Shown in Figure 3, F is a representative specimen concomitantly displaying in a single field bacteria lining the intervillous space, abutting the syncytiotrophoblast, and with greatest abundance in the villous parenchyma. These observations were all made in placental specimens from term birth, the majority of which were unlabored and delivered by cesarean (Figure 2, B). Nonetheless, similar localization within the placental microarchitecture was observed in placental specimens from preterm deliveries. As with their term counterparts, bacterial 16S rRNA signal was confidently visualized in the placental villous tissue of spontaneous preterm pregnancies both with and without ruptured membranes (Figure 4, A and B). Bacteria were similarly visualized and localized in the equivalent microarchitecture in placental specimens arising from unlabored cesarean births delivered in the preterm interval (Figure 4, C, arrows).

Systematic enumeration of whole sections of placental tissue from a random subset of subjects were exhaustively and manually analyzed at high power, using colony counting and estimation of size in an effort to establish a rough approximation of the visualized bacterial abundance. Estimates were highly heterogenous, both among subjects (intersubject variation) and within a single subject's placenta (intrasubject variation by subregions). Our best estimates included a range between 3 and ~200 bacteria per imaged slide, with the range of quantification variation appearing to be independent of gestational age at delivery, mode of delivery (cesarean vs vaginal), labor (labored or unlabored), and absence or presence of membrane rupture (all $P > .9$, data not shown). The most common characteristic among all subjects' specimens was the low abundance of these evidently low-biomass and sparse microbial communities. The relative density of bacteria within the placenta, as enumerated by estimating the typical volume of a given 4-μm section, was approximated to be $\sim 8 \times 10^4$ bacteria/cm^3 (SD $\pm$ 1.5 logs), 1–2 orders of magnitude greater than drinking water, and within a log-range of similar estimates for human breast milk.[75–78]

Detection of bacteria in pregnancies in term unlabored cesarean delivery

As shown in Figure 2 and described previously, a second cohort of unlabored, term cesarean deliveries were recruited and experimentally assessed by parallel clinical microbial cultivation, standard histologic measures, and 16S ISH. Clinical cultivation revealed no growth of bacteria in cord blood or aseptically sampled villous tissue for any placentas, including the small number of sPTB and a confirmed case of histologic and clinical evident chorioamnionitis. An environmental swab of the placental container, including the container vessel internal and external surfaces, the exterior handles, the ambient environment, and the absorbent underpad of the dissection surface, was also sent for clinical cultivation and, in all but 1 case, failed to yield clinically detectable bacterial growth (Figure 2, B). A single positive control (research personnel skin swab) grew *Staphylococci* within 48 hours. Despite the demonstrable absence of cultivatable bacteria under clinical microbiology protocols, evident 16S rRNA ISH signal was apparent in 18 of the 22 unlabored term placentas; the remaining 4 of 22 subjects' placentas had visualized signal potentially consistent with 16S rRNA staining but could not be adequately enumerated or distinguished from background. As detailed further in the Methods section, fluorescence labeling of 16S rRNA will occur among intact bacteria that are punctate and defined, highly amplified signal that partially preserves the morphology, intact placental bacteria that approach or exceed the morphologic resolution of light microscopy (eg, *Ureaplasma* and *Mycoplasma*), fragmented 16S rRNA, or artifacts of the sample processing that may resemble these. As with the placental specimens from preterm deliveries, bacterial signal was observed in the villous parenchyma, lining the intervillous space, and in proximity to the syncytiotrophoblast (Figure 5, arrows). Similarly, in all instances the presumptive microbial communities were sparse, focal, and of low abundance.

Comparative morphology employing Warthin–Starry bacterial stain

Standard clinical and histopathologic criteria were applied, and in no case (excepting the designated positive control) was there evidence of chorioamnionitis or intrauterine infection (Figure 2, B). As shown, ISH was superior in its sensitivity and specificity to WS, H&E, and Gram stain (Figure 6, Ai and Aii). Gram stain poorly differentiates bacteria from the background microarchitectural staining, particularly in the villous tissue, compared with the relatively acellular chorionic villi. When

A, Full cross-sections were formalin fixed and paraffin embedded for histologic studies while 16S gene sequencing was undertaken on sterilely dissected villous tissue. For the culture/cultivation cohort, villous tissue, venous and arterial cord blood samples, and environmental contamination control swabs were collected and sent for clinical culture and cultivation in a blinded fashion (red). **B,** A single case of chorioamnionitis was included, with the remainder of samples absent for confirmed or suspected clinical chorioamnionitis or intra-amniotic infection.

Seferovic et al. Visualization of placental microbiota. Am J Obstet Gynecol 2019.

we assessed serial sections with WS stain (histopathology stain historically used in diagnoses of tissue infection with bacteria such as *Spirochetes, Helicobacter pylori*, *Klebsiella*, and other small bacilli) with a clean silver nitrate–based contrast, WS staining enabled visualization of the largest colonies and all were inclusive of whole, unfragmented bacteria (Figure 6, iii and iv). Overall, though we were able to verify a few of the most abundant colonies of bacteria with WS staining, molecular histology employing ISH labeling of signal amplified 16S rRNA at high power was greatly superior in visualizing and localizing bacteria to the villous tree when compared with both WS and Gram stains.

Relative abundance estimates by 16S rRNA gene targeted amplicon sequencing distinguishes placental taxa as distinct from contaminant controls

To estimate the relative taxonomic abundance of bacterial genera, in parallel we performed 16S rRNA gene amplicon sequencing using primers targeting the V4 hypervariable region. Kit negative samples (DNA extraction blanks, absent of any biological tissue sample) and placentas from GF gnotobiotic mice were used as potential contamination controls. In total 63 samples were analyzed (ie, human placenta, GF mouse placenta, and DNA extraction blanks), with samples being lightly filtered (eg, chimeras were removed, but no removal of nonbacterial or unclassified bacterial ASVs was performed). In total, this approach generated 1,483,462 reads (average/median of 25,577/16,435 reads per sample) with minimum and maximum read counts of 3624 and 305,153, respectively. From these 16S metagenomic data we initially identified 1489 ASVs, corresponding to 356 genera. To compare the overall microbial community makeup (beta diversity), principal coordinate analysis on Bray-Curtis distances was undertaken at the phylum level for each of the 2 cohorts (Figure 7, A and B). We analyzed by cohort, and observed ordination separation in the largely preterm cohort when compared with contaminant controls (PERMANOVA, $R^2 = 0.083$, $P = .081$) (Figure 7, A). All placental metagenomes from largely term and unlabored cesarean births were significantly distinct in their clustering from contaminant controls

FIGURE 3
In situ visualized bacterial 16S rRNA signal in the term placenta

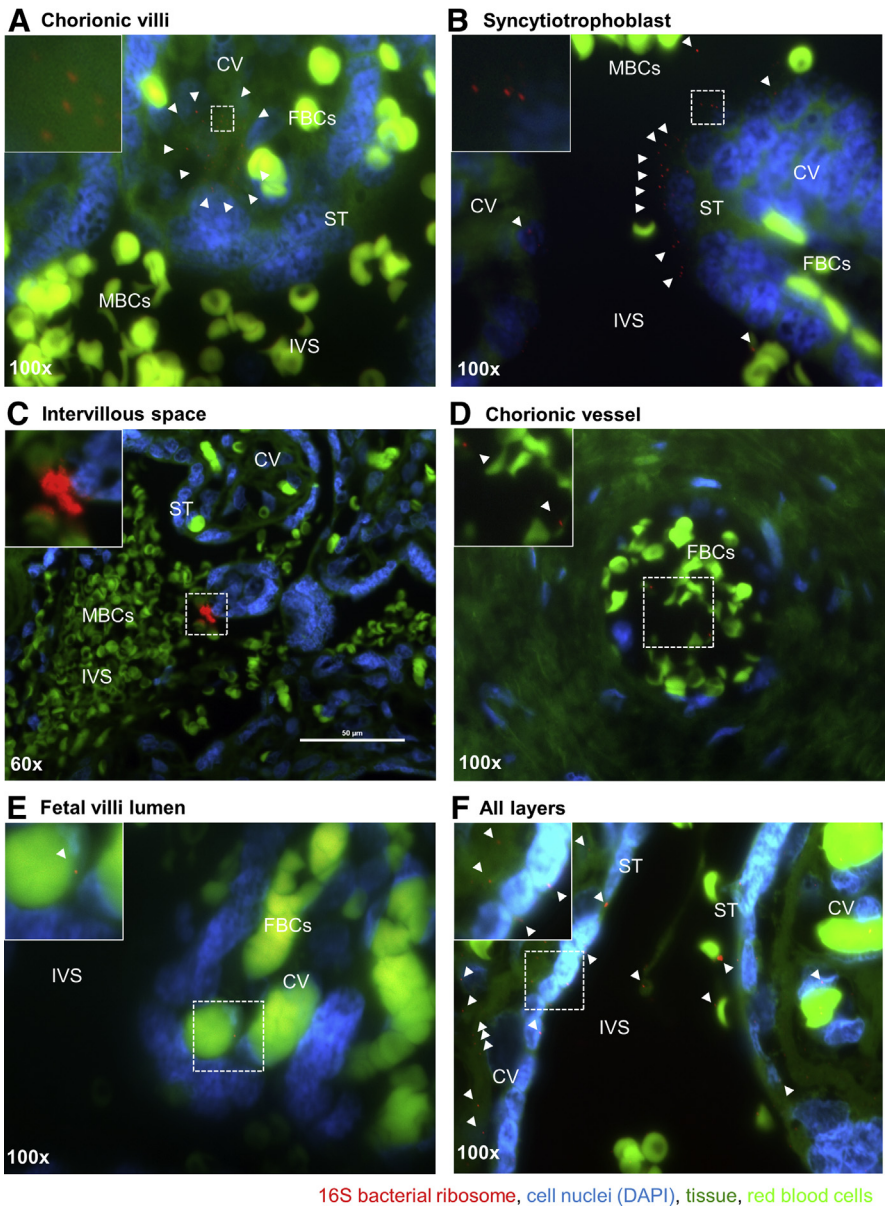

16S bacterial ribosome, cell nuclei (DAPI), tissue, red blood cells

Images taken from term controls (labored) show bacterial 16S rRNA signal (red) to occupy the villous parenchyma including **A,** the chorionic villi and **B,** in associated with the syncytiotrophoblast. Presumptive bacteria were seen in maternal and fetal circulation including commonly in **C,** the intervillous space, **D,** fetal chorionic vessels in 1 instance, and **E,** the fetal villi. **F,** All placental layers are represented in a single image from IVS to fetal vessels. Images shown are taken from 3 separate healthy term control patients: A,D,E from subject 1; C,F from subject 2; and B from subject 3. Boxed images show zoomed areas (dashed box).

CV, chorionic villi; *FBC*, fetal blood cells; *MBC*, maternal blood cells; *IVS*, intervillous space; *ST*, syncytiotrophoblast; (red: 16S rRNA; blue: DAPI; green: autofluorescence).

Seferovic et al. Visualization of placental microbiota. Am J Obstet Gynecol 2019.

FIGURE 4
In situ bacterial 16S rRNA signal in indicated and spontaneous preterm births

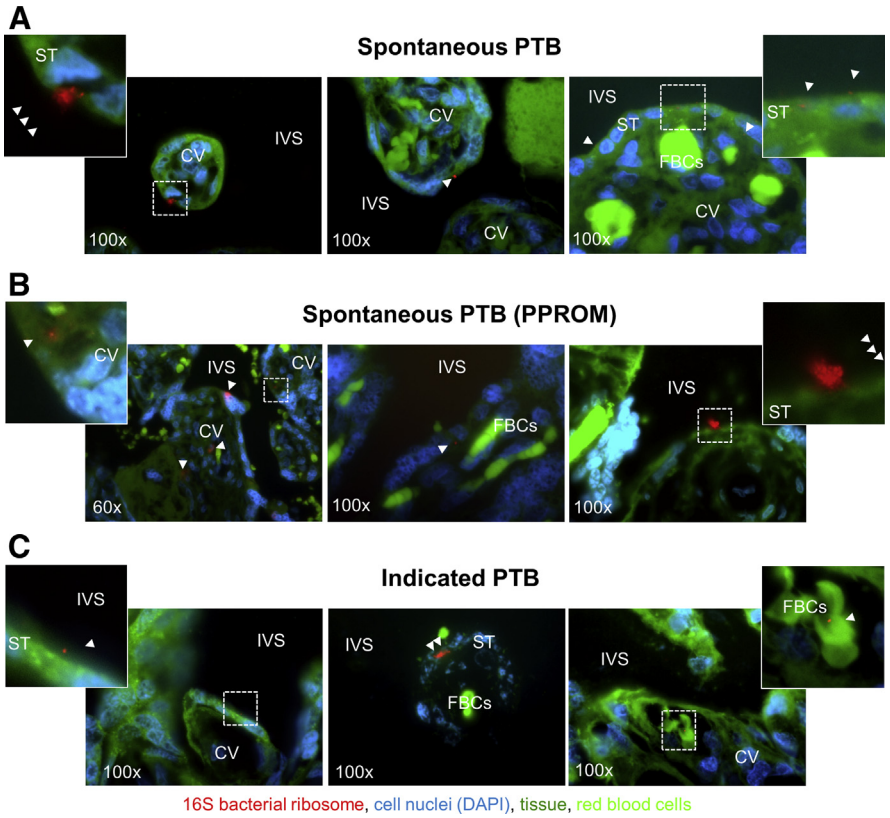

Representative images from **A,** 2 spontaneous preterm labor placentas, **B,** 2 spontaneous PTB with PPROM, and **C,** 3 indicated PTB placentas. Scarce 16S signal (red, arrows) was observed after careful systemic examination under high power in all but 5 PTB placentas examined. Boxed images show zoomed areas (dashed box).

CV, chorionic villi; *FBCs*, fetal blood cells; *IVS*, intervillous space; *PPROM*, preterm premature rupture of membranes; *PTB*, preterm birth; *ST*, syncytiotrophoblast; (red: 16S rRNA; blue: DAPI; green: tissue autofluorescence).

Seferovic et al. Visualization of placental microbiota. Am J Obstet Gynecol 2019.

(PERMANOVA, $R^2 = 0.06$, $P = .04$) (Figure 7, B). Phyla and genera were plotted by individual sample and group means (Figure 7, C and D, respectively). Overall, placental samples were predominated by phyla and their genera, as previously reported.[27–29,39–46,79–89] As anticipated, extraction kit negatives shared taxa with samples, particularly at the phylum level. A functional assessment of predicted pathway changes was also performed to examine for differences in population by function as plotted by sample and group (Figure 7, E). Over all there were 30 significant changes to relative predicted functional pathway enrichment between the kit negatives and placental samples (adjusted $P < .05$) (Appendix: Supplemental Table).

Computational identification and removal of putative contaminant taxonomic reads

To identify putative contaminant reads (as determined by ASVs), we performed prevalence-based filtering using the R package decontam.[71,72] In an effort to avoid any bias and enable completeness, we applied both decontam functions to the data, isContaminant (recommended for normal- to high-microbial-biomass samples) and isNotContaminant (recommended for low-microbial-biomass samples). isContaminant determined 58 ASVs to represent putative contaminants, and after removal of extraction blanks and samples with zero reads, 1297 ASVs remained across the 49 biological samples, which corresponded to 327 genera (Figure 8, A). The isNotContaminant function determined 1079 ASVs to represent putative contaminants (Figure 8, B). This resulted in the retention of 330 ASVs after removal of extraction blanks and samples with zero reads, which corresponded to 136 genera. Across the 49 placental samples, 731,832 decontaminated reads remained (average of 14,935 reads per sample) with minimum and maximum read counts of 1790 and 243,399, respectively. The isNotContaminant filtered data were used in subsequent analysis.

From the isNotContaminant filtered data we identified 28 genera that represent the top 10 genera from within term labored, term unlabored, spontaneous preterm, indicated preterm, PPROM, and chorioamnionitis cohorts (representing 72%, 80%, 76%, 82%, 90%, and 93% of each cohorts' overall genera, respectively) (Figure 8, C). Of these genera, 11 were determined to have significantly distinct distributions of relative abundance (Kruskal–Wallis test, $P < .05$), 5 of which remained significant after false discovery rate correction ($P < .05$). Post hoc analysis (Dunn's posttest, false discovery rate corrected, $P < .05$) revealed that in most cases there was no difference between term gestations, save for a higher abundance of *Abiotrophia* and *Neisseria* in placentas from unlabored term deliveries. However, there were community distinctions among preterm gestations. First, *Clostridium* spp were in abundance when comparing indicated with spontaneous preterm deliveries, suggesting a beyond week-of-gestational influence. Second, examination of differences between term and preterm placental specimens demonstrated variation in *Corynebacterium*, *Actinomyces*, *Veillonella*, *Streptococcus*, *Neisseria*, and *Finegoldia* abundances. However, these results and their taxonomic classifications need to be

FIGURE 5
In situ visualized bacterial 16S rRNA signal from exclusively term, cesarean-delivered placentas

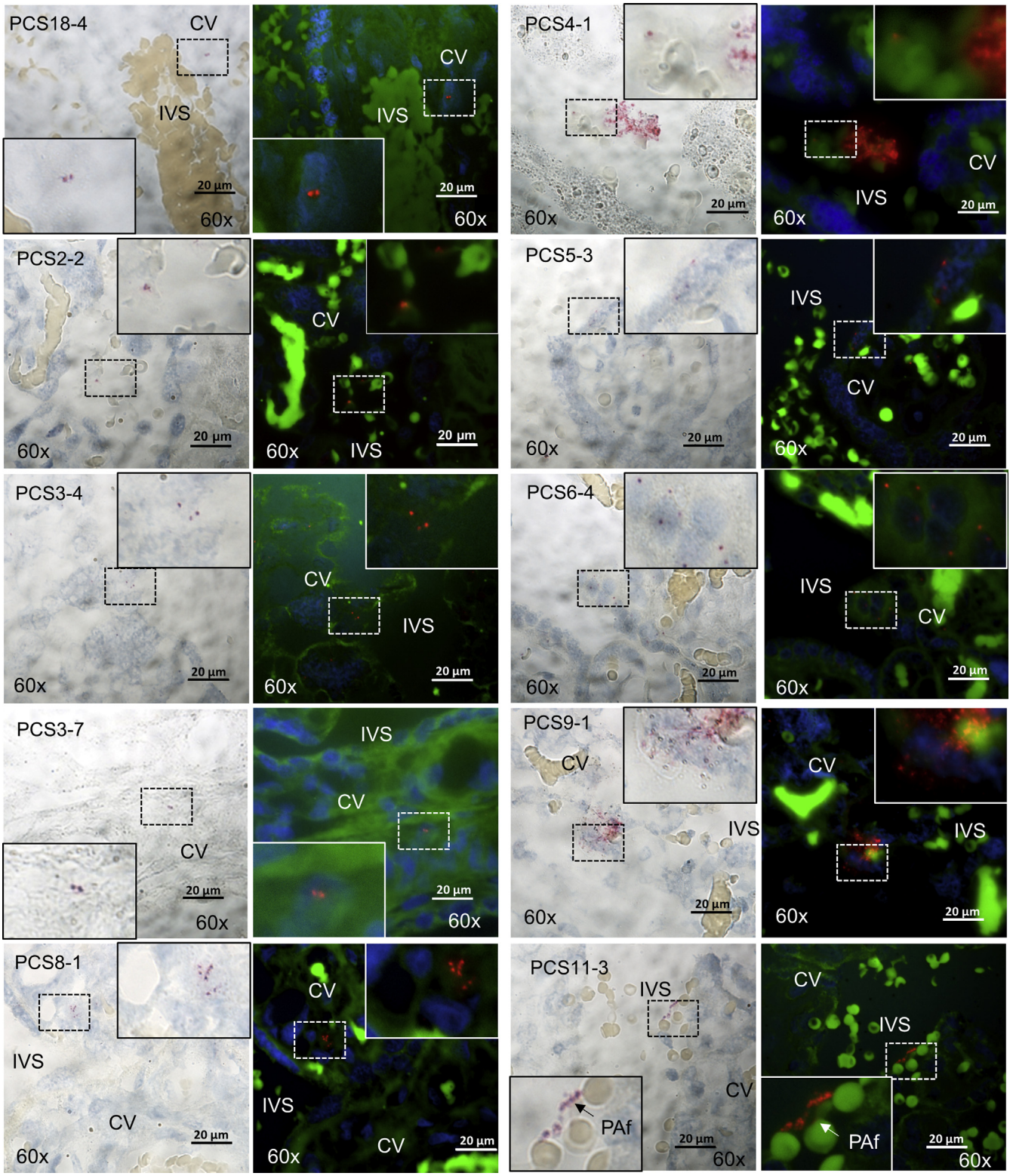

Seferovic et al. Visualization of placental microbiota. Am J Obstet Gynecol 2019.

(continued)

FIGURE 5
(*Continued*)

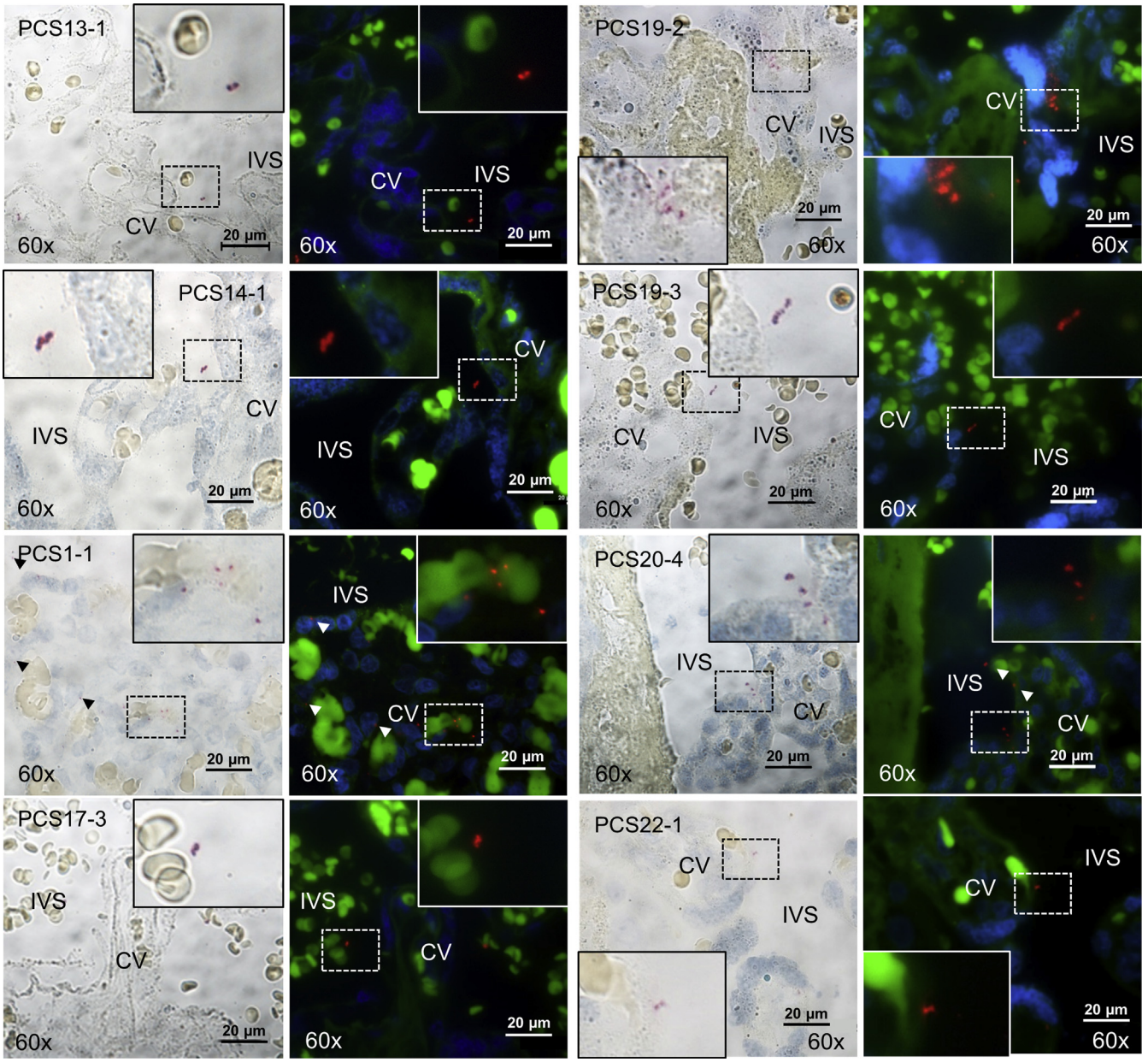

Paired, matching bright-field and fluorescent images showing 16S rRNA probe signal. Each image pair is of a separate placenta, with 1 for each of the 18 of 22 placentas examined where bacterial 16S rRNA signal was observed.

CV, chorionic villi; *IVS*, intervillous space; *PAf*, probably artifact; (red: 16S rRNA; blue: DAPI; green: autofluorescence).

Seferovic et al. Visualization of placental microbiota. Am J Obstet Gynecol 2019.

approached cautiously, since the majority of PTB were in the first subject cohort and the majority of term births were in the second subject cohort. Furthermore, differences in refined taxonomic assignments (ie, genus, species, or strain level) across studies reported for placenta and other low-biomass tissues are difficult to interpret and reservation should be given to assigning refined taxonomy based on short sequence reads. Given the diversity of massively parallel and next-generation sequencing platforms, methodologies, and choice of 16S variable regions for amplification, comparison across studies at refined levels should be approached with great caution.

FIGURE 6
Bacteria visualized with Warthin–Starry stain

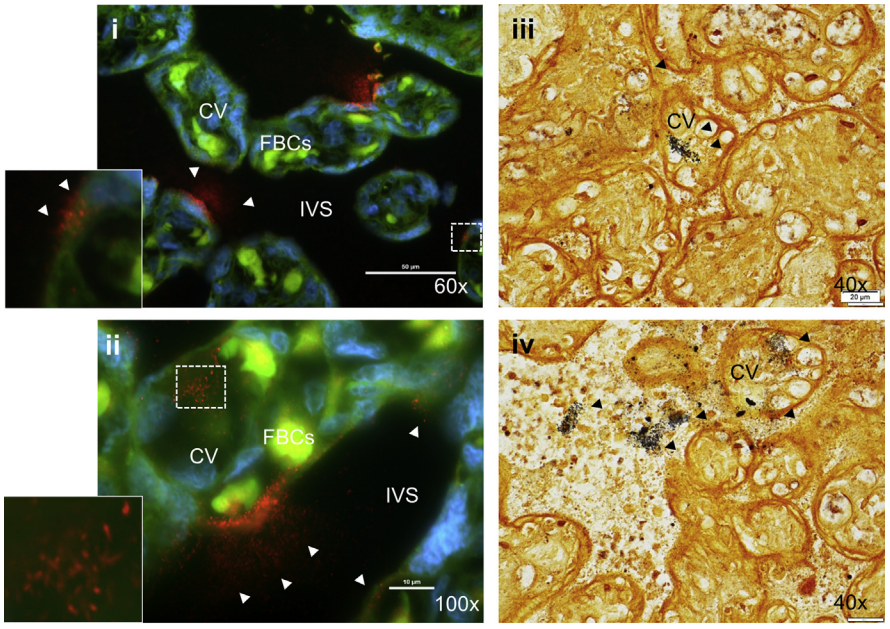

Large bacterial colonies at the center of the chorionic villi were observed by 16S probing and were revealed to be localized to an infarct of a placenta after hematoxylin–eosin examination (i,ii). The placenta was from a preterm delivery for preeclampsia without clinical or histologic chorioamnionitis. Despite the large amount of bacteria, none were detected by Gram stain in a blinded standard assessment. However, Warthin–Starry staining (used clinically to identify spirochetes) confirmed placental bacteria (iii,iv).

CV, chorionic villi; *IVS*, intervillous space; *FBCs*, fetal blood cells; (red: 16S rRNA; blue: DAPI; green:autofluorescence).

Seferovic et al. Visualization of placental microbiota. Am J Obstet Gynecol 2019.

Comment

Main findings

This report serves as the first detailed morphologic evidence employing 16S molecular in situ techniques demonstrating low-biomass populations of microbes that sparsely (but evidently) populate the human placenta. In the majority of placental specimens examined, 16S bacterial signal was apparent by high-power scanning microscopy using rRNA-based ribosome hybridization with branched DNA signal amplification. In agreement with previous histologic analyses, the subarchitectural localization of bacteria coincided in several instances with membrane stain–based detection and was consistent with presumptively intact bacteria.[17,18,24,26] However, in our hands 16S rRNA ISH with signal amplification was vastly superior with respect to confident detection and localization (further details are in Methods). We failed to observe quantitative differences in either the detection or localization of these communities when comparing term births and PTBs in the absence of clinical and histologic chorioamnionitis. However, we did observe heterogeneity of findings among and within individuals. Thus, we offer no definitive conclusions as to whether commensal microbial abundance varies by virtue of the preterm or term gestational interval. Nonetheless, we validate and expand upon our prior metagenomic-based estimates, and suggest that although of low biomass and low abundance with variability from one individual to the next, placental commensal microbiota are estimated to be at least 1–2 orders of magnitude greater than contaminated tap water.[77,78,90]

Comparison with existing literature and prior studies

Methods of detecting bacteria with morphology

Gram staining is based on dye-trapping within membranous structures.[60] Crystal violet preferentially precipitates with peptidoglycan structures, while safranin counterstains in red less robust structures (gram negative). Thus, although Gram stain is a well-known application for microbial detection, the dyes are not particularly specific for bacteria as they are more aptly tissue stains. For example, Gram stain is used in identifying mitotic figures in cells,[91] discriminating glial cells,[92] or identifying mast cells.[93] In this context, the limitations of Gram staining tissue are well known, with the original methodologic descriptions detailing the nonspecific effects of the 2 dyes (leukocytes and connective tissue stain red)[60,94–96] Similarly, the binding affinity to keratins[97] is what enables crystal violet to be used for surgical markings, and also makes it a prolific stain for the placental villous parenchyma, which is rich in cytokeratinous trophoblast cells.[98] It is therefore hardly surprising that in everyday use of crystal violet and Gram stains the rare bacteria would pass unnoticed on microscopic examination, unless in the presence of concomitant infection with inflammation and colony expansion. Similarly, it is also not surprising that others have shown that bacteria are detectable,[17,24,26] but only after applying laborious, manual systematic high-power microscopic examination, or when guided by clinical or histologic evidence of inflammation.

The use of WS stain made some bacteria very apparent, but only among the largest presumptive colonies (Figure 6, A) or instances where bacteria localized to acellular spaces (Figure 6, B). WS stain has been in use for the better part of a century, and is most often applied (as originally intended) for the detection of

FIGURE 7
Community profiling of placenta and environmental contaminants

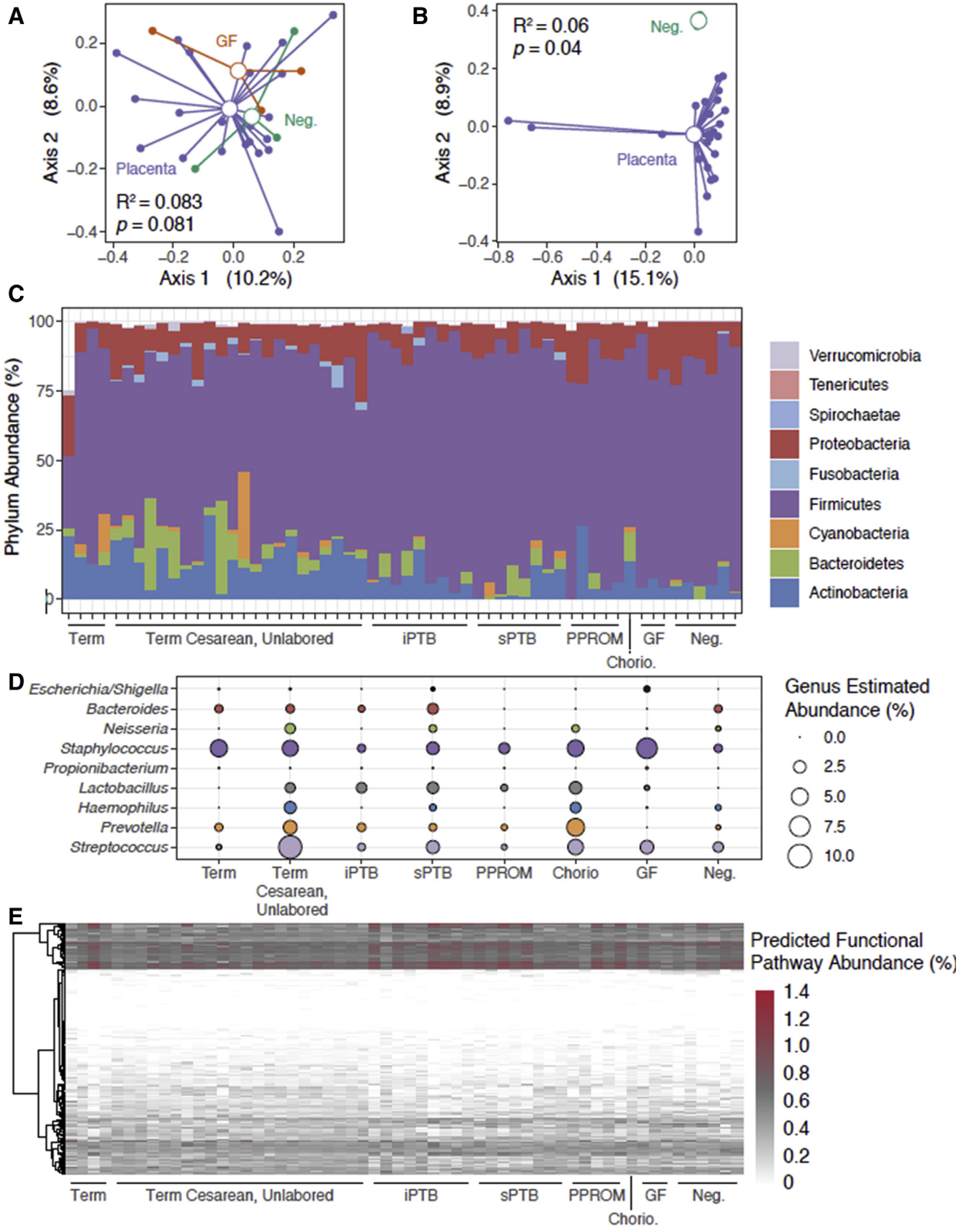

Spirochetes.[61] Like all silver stains, WS relies on the preferential deposition of silver nitrate, in this case onto cell walls, which are thereafter developed for contrast. Thus, like Gram stain, WS staining is not exquisitely specific, and the silver nitrate will deposit on microcalcifications, among other features in placenta.[99]

Morphologic analysis by standard FISH is similarly challenging in placenta, primarily owing to the autofluorescence of placental collagen, trophoblasts, and erythrocytes.[62–64] This is particularly true when attempting to discriminate fluorescent signal, which is nonubiquitous and focal, and therefore not readily apparent. Each of these occurrences necessitates long and laborious manual microscopic examination, during which time nonamplified and unstable signal is susceptible to quenching. We conclude that both Gram and WS staining techniques are summarily inferior in our hands and others'[17,18,26] to that of 16S rRNA ISH with stable signal amplification employing branched DNA technologies against the transcript. Notably, detection of bacteria in histologic chorioamnionitis is guided first by inflammation, not bacterial stains.

In several limited instances, the bacterial signal was densely clustered with radiating "halos" (Figure 6, A). For example, visualized microbes adjacent to and abutting the syncytiotrophoblast appear primarily lining the intervillous space and organized alongside the villous parenchyma (Figure 3). In many instances the bacteria were localized to the parenchyma, and were, in rare instances, associated with fetal vessels. Collectively, these findings would be most consistent with the observed microbes being largely from maternal sources, as suggested by our and other metagenomic characterizations.[16–18,27,29,31–34,41,45–50,52–55,79,80] Although such determination cannot be made in the current study and remains largely speculative, it is worthwhile noting that the colonies with the anticipated greatest numbers of microbes co-occurred with a placental infarct (Figure 6, A). Given the absence of blood supply in such an infarct, it is tempting to speculate that hematogenously spread bacteria would find refuge from maternal leukocytes or other phagosomes in such locations. Minor focal vascular defects, including small infarcts, are common and considered normal in ordinary pregnancy[81–83] but are more common in pregnancies affected by preeclampsia and fetal growth restriction. These observations are of interest given recent reports from other investigators that suggest metagenomic distinctions in placental communities occurs in cases of preeclampsia and fetal growth restriction, where infarcts of pathologic significance co-occur.[43,84]

Methods and limitations to detecting bacteria by cultivation

Aerobic bacteria have been cultured from the chorion in the absence of histologic chorioamnionitis,[31] and biopsies of the chorioamnion of mature placentas have revealed nearly half of placentas to be culture positive for diverse species.[16] This same study[16] recovered live *E. coli* from placenta, as did Onderdonk et al[25] from aseptically dissected villous parenchyma in preeclamptic pregnancies, placentas that were not expected to harbor microbes and, as with the current report, could not be explained by incidental or environmental contamination. We commend Collado et al[27] and others for their demonstrated ability to cultivate viable organisms including *Propionibacterium* and *Staphylococcus* from the placenta and amniotic fluid at the time of cesarean delivery in full-term pregnancies, and speculate that their ability to do so resulted from targeted approaches beyond current clinical microbiologic methodologies. Our inability to successfully culture bacteria from both the placentas and laboratory surfaces where there is no expectation of sterility is therefore expected and anticipated when using common current microbial culture techniques.[85–88] This may be particularly true with clinical cultivation methods, where techniques have been shaped to identify conventional pathogens rather than commensals, and the vast majority of strains are unculturable.[89,100,101]

Methods for detecting bacteria by sequencing

We were similarly not surprised by our metagenomic findings. Parallel 16S-based identification of course taxa (ie, at the phylum level) recapitulated our prior whole genome shotgun metagenomic findings[28,29,44] and characterized the placental microbiota detected as being composed of a unique community that could be distinguished from contaminant controls. In order to appropriately and rigorously analyze our 16S metagenomics data, a dual strategy of relevant environmental controls (Figure 7) and rigorous computational contaminant filtering has been developed and employed (Figure 8). As a result, our V4 amplicon 16S-based bacterial profiles are highly consistent with previous reports,[27–29,39,42–55] including our prior work with whole genome shotgun (non-amplicon-based) analysis.[28,29,44] Thus, distinct from 2 groups' conclusions,[46,48,58] but consistent with numerous others[16–18,27,29,31–34,41,45–50,52–55,74,75] we

A,B, Differences in microbial community composition (beta diversity) were assessed by Bray-Curtis dissimilarity for each of the 2 cohorts. Closed circles represent samples with colored lines traced back to open circles that represent centroids. Placental samples are shaded purple, germ-free mouse placenta are shaded orange, and extraction blank kit negatives are shaded green. **C,** The mean relative unfiltered abundance of bacterial phyla (amplicon sequence variant assignments) is plotted for each sample by group. **D,** Differences in bacterial genera abundance by mean are plotted. **E,** Group differences by predicted pathways as assessed by PICRISt2 from amplicon sequence variants; 30 were enriched or depleted significantly after correction for multiple comparisons (Supplemental Table 1).

chorio, chorioamnionitis; *neg*, kit negative controls; *GF*, germ free; *iPTB*, medically indicated preterm birth; *PPROM*, preterm premature rupture of membranes; *sPTB*, spontaneous preterm birth.

Seferovic et al. Visualization of placental microbiota. Am J Obstet Gynecol 2019.

FIGURE 8
Prevalence-based decontamination reveals community differences among term and preterm placentas

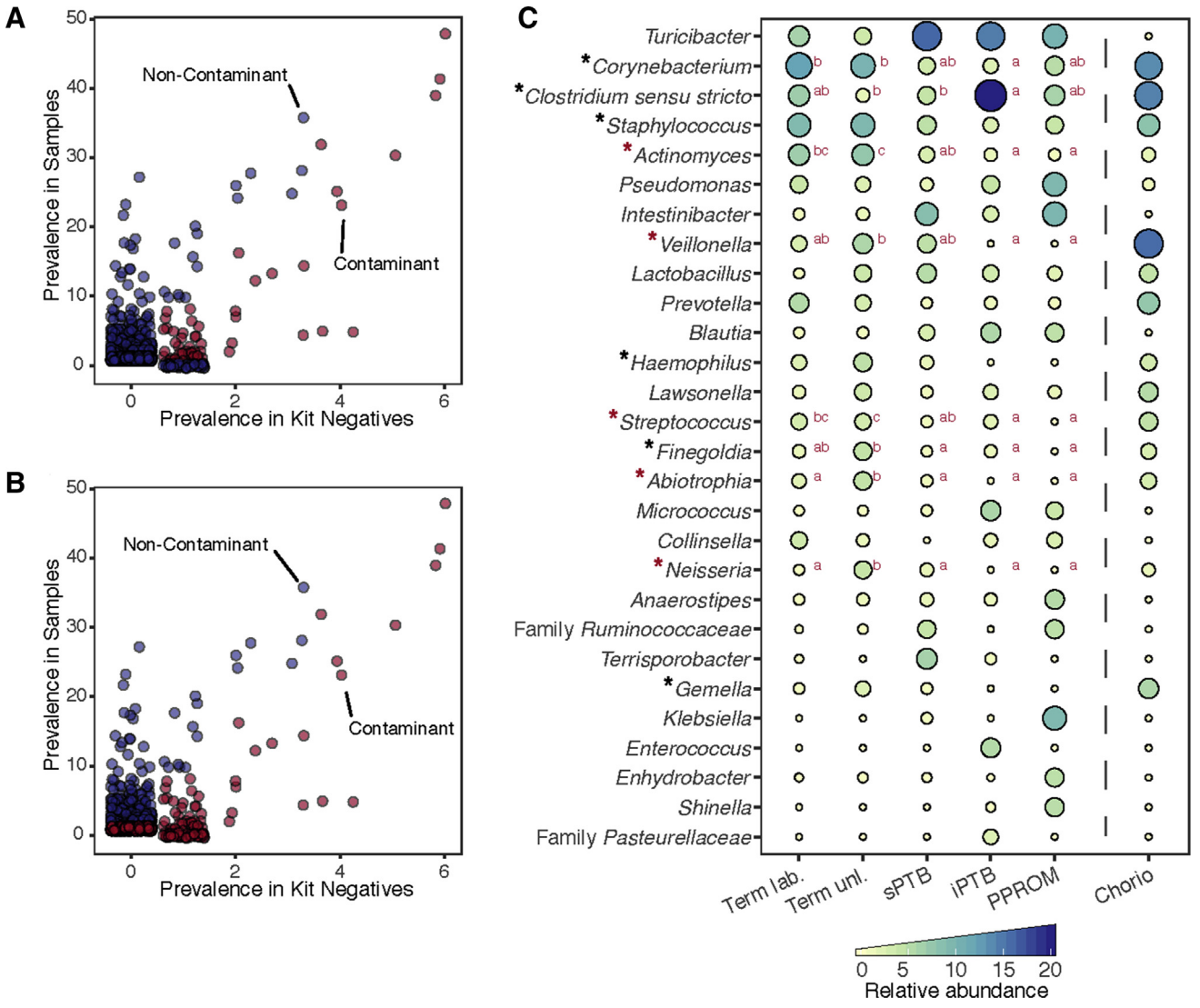

A, Prevalence plot of amplicon sequence variants (ASVs) statistically determined to be noncontaminants or contaminants as determined by the decontam isContaminant function. Fifty-eight ASVs were found to have statistical support that indicated they represent putative contaminants. ASVs determined to be contaminants are shaded red, whereas ASVs determined to be noncontaminants are shaded blue. **B,** Prevalence plot of ASVs statistically determined to be noncontaminants or contaminants as determined by the decontam isNotContaminant function—recommended for low-microbial-biomass sample types. isNotContaminant tests the hypothesis that ASVs have statistical support showing they represent valid ASVs that originate from within the biological samples as opposed to the extraction blank negative controls. A total of 330 ASVs were found to have statistical support that indicated they represent true ASVs. The increase in putative contaminant ASVs identified by isNotContaminant compared to isContaminant arises largely from ASVs present in only a single sample. Contaminant and noncontaminant ASVs are shaded as in panel A. **C,** The 10 most abundant genera from within each sample type after decontam filtering. Significant differences between sample types were determined via Kruskal—Wallis test (black asterisks indicate $P < .05$, red asterisks indicate false discovery rate—corrected $P < .05$), followed by Dunn's posttest for differences between groups (red letters indicate significance groups, $P < .05$).

chorio, chorioamnionitis; *iPTB*, medically indicated preterm birth; *PPROM*, preterm premature rupture of membranes; *sPTB*, spontaneous preterm birth.

Seferovic et al. Visualization of placental microbiota. Am J Obstet Gynecol 2019.

find that 16S rRNA sequencing—based detection of placental microbes is not the mere product of environmental or ambient contamination but rather represents the same low-biomass, low-abundance community we visually observe with 16S rRNA ISH. The primary difference between our studies and those of others[56,58] is the choice of 16S amplicon primers used: the laboratory of Bushman (Lauder et al[56] and Leiby et al[59]) utilized 16S V1—V2 region primers, whereas we

and others use standard 16S V4 region primers. Selection of variable region selection and primer conditions influence the capacity to separate communities compared to a naïve WGS approach, and this truth likely extends to "contaminated" populations. We concur that there both should be and are shared taxa (as measured by 16S-based amplicons) between the environment and any extracted sample. This in fact reaffirms our previously voiced cautions[29] and those of others[56–58,102] to carefully consider and control for environmental contaminants when working with low-microbial-biomass samples. However, it is equally important to emphasize that shared taxa does not a community of contaminants make.

Strengths and limitations of our approach and study

Our study used a combination of state-of-the-science imaging techniques and sequencing approaches to overcome technical limitations. Compared with conventional staining, amplified probes with diligent, tedious, and systematic manual microscopic approaches were better able to detect bacteria when attempting to visualize in situ against the placental microarchitecture. Further, our 16S-based sequencing pipeline used here was the beneficiary of techniques and improvements gleaned in recent years, where we used relevant V4 primer sets and ASV-based taxonomic assignments together with recently developed data decontamination techniques. Collectively this is a vast improvement over other published 16S-based placental assessments. In the current study, these assessments expectantly revealed that although there is overlapping taxonomic membership, the majority of reads detected here are unique to the placenta and thus distinguish the community from environmental contamination controls. Although further contamination filtering increased the significance of clustering, it was not necessary to differentiate the taxonomic makeup, indicating the limited influence of low-level contaminants, which will be inherent to any microbial community analyzed by metagenomics, but proportionally greater in low-biomass communities such as the skin, placenta, human breast milk, and neonatal stool.

In this study we were able to visualize and localize bacteria using specific probes sets and branched DNA amplification for stable signal that associates with the recently synthesized cytoplasmic rRNA of the intact organism. This is notably different from our and others' previous metagenomics sequencing-based characterizations of the stable gene.[27–29,39,42–45] The specificity of the probes to intracellular bacterial ribosomes and the inherent incompatibility of hybridizing with double-stranded DNA fragments is a notable strength.[103] The concomitant lack of inflammation as observed by H&E staining suggests that these bacteria are unlikely to represent a latent or nascent infection, which is further supported by the observation that the identified bacteria were not found in association to phagocytes. The inability to ubiquitously visualize microbiota with standard Gram staining guided by H&E (Figure 2, B), even in high villus concentration (Figure 6, A), exemplifies the technical problem of identifying rare bacteria in heterogeneous tissue with poor discrimination resulting from cellular stain.[94–96]

Despite evident and multiple strengths, our study has several inherent limitations. First, we are confined by the intrinsically small tissue volumes that can be analyzed by high-powered microscopy with fluorescent labels, and are thus left to infer planar localization and concentrations of bacteria as being relatively uniform across a large and diverse organ. Despite our best efforts to control for sources of contamination, in the absence of any known true "sterile tissue" there is inherent risk of misidentification of bacterial signal in high- and low-biomass specimens alike. Histologic work, like metagenomic sequencing, may be influenced by the inherent and, thus far, unavoidable trace reagent contamination.[17,18,26] Given that control cases (unlabored term cohort) are more similar to other placental samples than contaminant controls, a true "negative control" for ours (or any such study) remains elusive. It is possible, despite ardent efforts to avoid doing so and side-by-side comparisons to bright fields, that we have misinterpreted autofluorescence as 16S rRNA–specific signal. Although we have been conservative in what we ultimately deemed labeled bacterial "signal" and what we deemed "likely artifact," it remains a possibility that we have overestimated true bacterial signal. Indeed with a generic 16S probe, contamination and artifacts are conceivably related. Further, highly amplified signals have diminished morphologic preservation, which, when compounded by sheer size and biomass limitations, makes bacterial resolution and discrimination against background findings very technically challenging in the placenta. The equivalent of a tissue section's volume of breast milk ($\sim$0.5 μL) would contain only $\sim$5 bacteria.[75,76] Stated differently, observed bacteria occupy a hundred millionth ($1/10^8$) of the relative placental volume. Nevertheless, they are present.

Conclusions and implications

Collectively, our findings reported herein document a low but consistently observable biomass of bacteria in the placental villous tissue that are taxonomically distinct from potential environmental contamination controls. These bacteria appear present in the majority of placenta assessed, regardless of mode of delivery, gestational age, or occurrence of labor. We summarily conclude that presumptively intact placental bacteria are sparse but predictable in their occurrence and localization within the placental microarchitecture. This would collectively ascribe the community as being one of low abundance and low biomass, consistent with the conclusions of multiple previous metagenomic studies from term and preterm placental specimens.

With respect to the conclusions that can be drawn by the state of scientific evidence, we remain agnostic as to whether this is a community that is live and colonizing, or rather a highly predictable and consistent collection of

metagenomes that may or may not be alive (eg, harboring a unique microbiome, viability unknown). Neither this study nor our other publications[28,29,32,44] have formally tested the viability of these organisms, but they do acknowledge that other investigators have successfully done so. We similarly make no definitive conclusions regarding either the origin or the fate of these presumptive microbiome constituents. Although we have published previously the degree of taxonomic similarity between the placental and oral metagenomic communities, these were reported as cross-sectional comparisons from different cohorts.[29] Moreover, we have consistently iterated that the placental metagenomics community is of low biomass and low abundance, and its diversity does not nearly approximate that of the oral or any other relatively higher-biomass community; the current study does not further or refute our prior observations.[28,29,44] Finally, though we are enthused with the emerging findings of others pertaining to evidence suggesting immune maturation and tolerance in the human fetus,[51] it is as of yet unclear whether this is a consequence of noninherited maternal HLA antigens or bacterial-derived ligands and antigens from the placenta, amniotic fluid, or membranes. Regardless of the viability (or lack thereof) of these metagenomics communities, we continue to concur that immune priming during fetal life would be fundamentally crucial and important for the tolerance of the massive influx of bacteria that are encountered ex utero.[29,32,51]

The potential implications of our findings to the practicing clinician are several. Firstly, the finding of bacteria in the placenta is further evidence against the assumption of true "sterility" of the gestational milieu. We speculate that this may have implications for potential in utero seeding and/or establishment of immunologic tolerance during fetal life. Secondly, our findings, combined with those of others, suggest that largely historical practices of culturing or cultivating placental specimens for bacteria taken at the time of delivery are unlikely to yield clinically actionable information and are thus of little or no value. Alternately, our observations support the current practice of reserving the diagnosis of intraamniotic infection based on clinical criteria of fever, uterine tenderness, maternal tachycardia, and fetal tachycardia or with amniocentesis documenting concern for immune expansion or viable organisms. ■

Acknowledgements

The authors which to acknowledge Drs Christopher Stewart and Michelle Moller for their contributions to 16S rRNA sequencing and analysis, as well as subject recruitment.

References

1. Saigal S, Doyle LW. An overview of mortality and sequelae of preterm birth from infancy to adulthood. Lancet 2008;371:261–9.
2. Sadowsky DW, Novy MJ, Witkin SS, Gravett MG. Dexamethasone or interleukin-10 blocks interleukin-1beta-induced uterine contractions in pregnant rhesus monkeys. Am J Obstet Gynecol 2003;188:252–63.
3. Romero R, Mazor M, Tartakovsky B. Systemic administration of interleukin-1 induces preterm parturition in mice. Am J Obstet Gynecol 1991;165:969–71.
4. Grigsby PL, Hirst JJ, Scheerlinck J-P, Phillips DJ, Jenkin G. Fetal responses to maternal and intra-amniotic lipopolysaccharide administration in sheep. Biol Reprod 2003;68:1695–702.
5. Gravett MG, Witkin SS, Haluska GJ, Edwards JL, Cook MJ, Novy MJ. An experimental model for intraamniotic infection and preterm labor in rhesus monkeys. Am J Obstet Gynecol 1994;171:1660–7.
6. Grigsby PL, Novy MJ, Sadowsky DW, et al. Maternal azithromycin therapy for Ureaplasma intraamniotic infection delays preterm delivery and reduces fetal lung injury in a primate model. Am J Obstet Gynecol 2012;207:475.e1–14.
7. Trivedi S, Joachim M, McElrath T, et al. Fetal-placental inflammation, but not adrenal activation, is associated with extreme preterm delivery. Am J Obstet Gynecol 2012;206:236.e1–8.
8. Buhimschi CS, Dulay AT, Abdel-Razeq S, et al. Fetal inflammatory response in women with proteomic biomarkers characteristic of intra-amniotic inflammation and preterm birth. BJOG 2009;116:257–67.
9. Shim S-S, Romero R, Hong J-S, et al. Clinical significance of intra-amniotic inflammation in patients with preterm premature rupture of membranes. Am J Obstet Gynecol 2004;191:1339–45.
10. Combs CA, Gravett M, Garite TJ, et al. Amniotic fluid infection, inflammation, and colonization in preterm labor with intact membranes. Am J Obstet Gynecol 2014;210:125.e1–15.
11. DiGiulio DB, Romero R, Amogan HP, et al. Microbial prevalence, diversity and abundance in amniotic fluid during preterm labor: a molecular and culture-based investigation. PLoS One 2008;3(8):e3056.
12. Romero R, Gomez R, Ghezzi F, et al. A fetal systemic inflammatory response is followed by the spontaneous onset of preterm parturition. Am J Obstet Gynecol 1998;179(1):186–93.
13. Romero R, Mazor M. Infection and preterm labor. Clin Obstet Gynecol 1988;31(3):553–84.
14. Agrawal V, Hirsch E. Intrauterine infection and preterm labor. Semin Fetal Neonatal Med 2012;17:12–9.
15. Kim MJ, Romero R, Gervasi MT, et al. Widespread microbial invasion of the chorioamniotic membranes is a consequence and not a cause of intra-amniotic infection. Lab Invest 2009;89:924–36.
16. Pettker CM, Buhimschi IA, Magloire LK, Sfakianaki AK, Hamar BD, Buhimschi CS. Value of placental microbial evaluation in diagnosing intra-amniotic infection. Obstet Gynecol 2007;109:739–49.
17. Stout MJ, Conlon B, Landeau M, et al. Identification of intracellular bacteria in the basal plate of the human placenta in term and preterm gestations. Am J Obstet Gynecol 2013;208:226.e1–7.
18. Steel JH, Malatos S, Kennea N, et al. Bacteria and inflammatory cells in fetal membranes do not always cause preterm labor. Pediatr Res 2005;57:404–11.
19. Hillier SL, Martius J, Krohn M, Kiviat N, Holmes KK, Eschenbach DA. A case-control study of chorioamnionic infection and histologic chorioamnionitis in prematurity. N Engl J Med 1988;319:972–8.
20. Cassell GH, Davis RO, Waites KB, et al. Isolation of Mycoplasma hominis and Ureaplasma urealyticum from amniotic fluid at 16-20 weeks of gestation: potential effect on outcome of pregnancy. Sex Transm Dis 2015;10(4 Suppl):294–302.
21. Romero R, Miranda J, Chaemsaithong P, et al. Sterile and microbial-associated intra-amniotic inflammation in preterm prelabor rupture of membranes. J Matern Fetal Neonatal Med 2015;28:1394–409.
22. Romero R, Miranda J, Chaiworapongsa T, et al. Sterile intra-amniotic inflammation in asymptomatic patients with a sonographic short cervix: prevalence and clinical significance. J Matern Fetal Neonatal Med 2014;28:1–17.
23. Romero R, Miranda J, Kusanovic JP, et al. Clinical chorioamnionitis at term I: microbiology of the amniotic cavity using cultivation and molecular techniques. J Perinat Med 2015;43:19–36.
24. Cao B, Mysorekar IU. Intracellular bacteria in placental basal plate localize to extravillous trophoblasts. Placenta 2014;35:139–42.

25. Onderdonk AB, Delaney ML, DuBois AM, Allred EN, Leviton A. Detection of bacteria in placental tissues obtained from extremely low gestational age neonates. Am J Obstet Gynecol 2008;198:110.e1–7.

26. Parnell LA, Briggs CM, Cao B, Delannoy-Bruno O, Schrieffer AE, Mysorekar IU. Microbial communities in placentas from term normal pregnancy exhibit spatially variable profiles. Sci Rep 2017;7:11200.

27. Collado MC, Rautava S, Aakko J, Isolauri E, Salminen S. Human gut colonisation may be initiated in utero by distinct microbial communities in the placenta and amniotic fluid. Sci Rep 2016;6:23129.

28. Prince AL, Ma J, Kannan PS, et al. The placental membrane microbiome is altered among subjects with spontaneous preterm birth with and without chorioamnionitis. Am J Obstet Gynecol 2016;214:627.e1–16.

29. Aagaard K, Ma J, Antony KM, Ganu R, Petrosino J, Versalovic J. The placenta harbors a unique microbiome. Sci Transl Med 2014;6:237–65.

30. Ardissone AN, de la Cruz DM, Davis-Richardson AG, et al. Meconium microbiome analysis identifies bacteria correlated with premature birth. PLoS One 2014;9(3):e90784.

31. Kovalovszki L, Villányi Z, Pataki I, Veszelowvsky I, Nagy ZB. Isolation of aerobic bacteria from the placenta. Acta Paediatr Acad Sci Hung 1982;23:357–60.

32. Chu DM, Ma J, Prince AL, Antony KM, Seferovic MD, Aagaard KM. Maturation of the infant microbiome community structure and function across multiple body sites and in relation to mode of delivery. Nat Med 2017;23:314–26.

33. Mshvildadze M, Neu J, Shuster J, Theriaque D, Li N, Mai V. Intestinal microbial ecology in premature infants assessed with non-culture-based techniques. J Pediatr 2010;156:20–5.

34. Moles L, Gómez M, Heilig H, et al. Bacterial diversity in meconium of preterm neonates and evolution of their fecal microbiota during the first month of life. PLoS One 2013;8:e66986.

35. Horowitz S, Mazor M, Romero R, Horowitz J, Glezerman M. Infection of the amniotic cavity with Ureaplasma urealyticum in the midtrimester of pregnancy. J Reprod Med 1995;40(5):375–9.

36. Nguyen DP, Gerber S, Hohlfeld P, Sandrine G, Witkin SS. Mycoplasma hominis in mid-trimester amniotic fluid: relation to pregnancy outcome. J Perinat Med 2004;32:323–6.

37. Romero R, Nores J, Mazor M, et al. Microbial invasion of the amniotic cavity during term labor. Prevalence and clinical significance. J Reprod Med 1993;38:543–8.

38. Goldenberg RL, Culhane JF, Iams JD, Romero R. Epidemiology and causes of preterm birth. Lancet 2008;371:75–84.

39. Zheng J, Xiao X, Zhang Q, Mao L, Yu M, Xu J. The placental microbiome varies in association with low birth weight in full-term neonates. Nutrients 2015;7:6924–37.

40. Onderdonk AB, Hecht JL, McElrath TF, Delaney ML, Allred EN, Leviton A. Colonization of second-trimester placenta parenchyma. Am J Obstet Gynecol 2008;199:52.e1–10.

41. Jiménez E, Fernández L, Marín ML, et al. Isolation of commensal bacteria from umbilical cord blood of healthy neonates born by cesarean section. Curr Microbiol 2005;51:270–4.

42. Doyle RM, Alber DG, Jones HE, et al. Term and preterm labour are associated with distinct microbial community structures in placental membranes which are independent of mode of delivery. Placenta 2014;35:1099–101.

43. Amarasekara R, Jayasekara RW, Senanayake H, Dissanayake VHW. Microbiome of the placenta in pre-eclampsia supports the role of bacteria in the multifactorial cause of pre-eclampsia. J Obstet Gynaecol Res 2015;41:662–9.

44. Antony KM, Ma J, Mitchell KB, Racusin DA, Versalovic J, Aagaard K. The preterm placental microbiome varies in association with excess maternal gestational weight gain. Am J Obstet Gynecol 2015;212:653.e1–16.

45. Gardella C, Riley DE, Hitti J, Agnew K, Krieger JN, Eschenbach D. Identification and sequencing of bacterial rDNAs in culture-negative amniotic fluid from women in premature labor. Am J Perinatol 2004;21:319–23.

46. Bassols J, Serino M, Carreras-Badosa G, et al. Gestational diabetes is associated with changes in placental microbiota and microbiome. Pediatr Res 2016;80:777–84.

47. Doyle RM, Harris K, Kamiza S, et al. Bacterial communities found in placental tissues are associated with severe chorioamnionitis and adverse birth outcomes. PLoS One 2017;12:e0180167.

48. Gomez-Arango LF, Barrett HL, McIntyre HD, Callawy LK, Morrison M, Nitert MD. Contributions of the maternal oral and gut microbiome to placental colonization in overweight and obese pregnant women. Sci Rep 2017;7:2860.

49. Zheng J, Xiao XH, Zhang Q, et al. Correlation of placental microbiota with fetal macrosomia and clinical characteristics in mothers and newborns. Oncotarget 2017;8:82314–25.

50. Leon LJ, Doyle R, Deiz-Benavente E, et al. Enrichment of clinically relevant organisms in spontaneous preterm delivered placenta and reagent contamination across all clinical groups in a large UK pregnancy cohort. Appl Environ Microbiol 2018;84:14.

51. Li N, van Unen V, Abdelaal T, et al. Memory CD4+ T cells are generated in the human fetal intestine. Nat Immunol 2019;20:301–12.

52. Satokari R, Gronoroos T, Laitinen K, Salmine S, Isolauri E. Bifidobacterium and Lactobacillus DNA in the human placenta. Lett Appl Microbiol 2009;48:8–12.

53. Rautava S, Collado MC, Salminen S, Isolauri E. Probiotics modulate host-microbe interaction in the placenta and fetal gut: a randomized, double-blind, placebo-controlled trial. Neonataology 2012;102:178–84.

54. Martinez KA, Romano-Keeler J, Zackular JP, et al. Bacerial DNA is present in the fetal intestine and overlaps with that in the placenta in mice. PLoS One 2018;13(5):e0197439.

55. Borghi E, Massa V, Severgnini M, et al. Antenatal microbial colonization of mammalian gut. Reprod Sci 2018:1933719118804411.

56. Lauder AP, Roche AM, Sherrill-Mix S, et al. Comparison of placenta samples with contamination controls does not provide evidence for a distinct placenta microbiota. Microbiome 2016;4:29.

57. Salter SJ, Cox MJ, Turek EM, et al. Reagent and laboratory contamination can critically impact sequence-based microbiome analyses. BMC Biol 2014;12:87.

58. Theis KR, Romero R, Winters AD, et al. Does the human placenta delivered at term have a microbiota? Results of cultivation, quantitative real-time PCR, 16S rRNA gene sequencing, and metagenomics. Am J Obstet Gynecol 2019:267.e1.

59. Leiby JS, McCormick K, Sherrill-Mix S, et al. Lack of detection of a human placenta microbiome in samples from preterm and term deliveries. Microbiome 2018;6:196.

60. Taylor RD. Modification of the Brown and Brenn gram stain for the differential staining of gram-positive and gram-negative bacteria in tissue sections. Am J Clin Pathol 1966;46:472–4.

61. Warthin AS, Starry A. A more rapid and improved method of demonstrating spirochetes in tissues. Am J Syph 1920;4:97–103.

62. Erlebacher A, Lukens AK, Glimcher LH. Intrinsic susceptibility of mouse trophoblasts to natural killer cell-mediated attack in vivo. Proc Natl Acad Sci U S A 2002;99:16940–5.

63. Aagaard KM, Lahon A, Suter MA, et al. Primary human placental trophoblasts are permissive for zika virus (ZIKV) replication. Sci Rep 2017;7:41389.

64. Merz G, Schwenk V, Shah RG, Necaise P, Salafia CM. Clarification and 3-D visualization of immunolabeled human placenta villi. Placenta 2017;53:36–9.

65. Battich N, Stoeger T, Pelkmans L. Image-based transcriptomics in thousands of single human cells at single-molecule resolution. Nat Methods 2013;10(11):1127–33.

66. Martin M. Cutadapt removes adapter sequences from high-throughput sequencing reads. EMBnet.journal 2011;17:10.

67. Bolger AM, Lohse M, Usadel B. Trimmomatic: a flexible trimmer for Illumina sequence data. Bioinformatics 2014;30:2114–20.

68. Callahan BJ, McMurdie PJ, Rosen MJ, Han AW, Johnson AJA, Holmes SP. DADA2: High-resolution sample inference from Illumina amplicon data. Nat Methods 2016;13:581–3.

69. McMurdie PJ, Holmes S. phyloseq: An R package for reproducible interactive analysis and graphics of microbiome census data. PLoS One 2013;8:e61217.

70. Langille MGI, Zaneveld J, Caporaso JG, et al. Predictive functional profiling of microbial communities using 16S rRNA marker gene sequences. Nat Biotechnol 2013;31:814–21.
71. Davis NM, Proctor D, Holmes SP, Relman DA, Callahan BJ. Simple statistical identification and removal of contaminant sequences in marker-gene and metagenomics data. bioRxiv 2018;221499.
72. Davis NM, Proctor DM, Holmes SP, Relman DA, Callahan BJ. Simple statistical identification and removal of contaminant sequences in marker-gene and metagenomics data. Microbiome 2018;6:226.
73. J O, et al. Vegan: Community Ecology Package. Ordination Methods, Diversity Analysis and Other Functions for Community and Vegetation Ecologists. http://outputs.worldagroforestry.org/cgi-bin/koha/opac-detail.pl?biblionumber=39504. Accessed March 14, 2019.
74. Wickham H. Ggplot2: Elegant Graphics for Data Analysis. New York, NY: Springer; 2009.
75. Heikkilä MP, Saris PEJ. Inhibition of Staphylococcus aureus by the commensal bacteria of human milk. J Appl Microbiol 2003;95:471–8.
76. Pittard WB, Geddes KM, Brown S, Mintz S, Hulsey TC. Bacterial contamination of human milk: container type and method of expression. Am J Perinatol 1991;8:25–7.
77. Lalumandier JA, Ayers LW. Fluoride and bacterial content of bottled water vs tap water. Arch Fam Med 2000;9:246–50.
78. Harnroongroj T, Leelaporn A, Limsrivanichayakorn S, Kaewdaeng S, Harnroongroj T. Comparison of bacterial count in tap water between first burst and running tap water. J Med Assoc Thai 2012;95:712–5.
79. Jiménez E, Marín ML, Martín R, et al. Is meconium from healthy newborns actually sterile? Res Microbiol 2008;159:187–93.
80. Han YW, Shen T, Chung P, Buhimschi IA, Buhimschi CS. Uncultivated bacteria as etiologic agents of intra-amniotic inflammation leading to preterm birth. J Clin Microbiol 2009;47:38–47.
81. Becroft DMO, Thompson JMD, Mitchell EA. The epidemiology of placental infarction at term. Placenta 2002;23:343–51.
82. Beauharnais CC, Roberts DJ, Wexler DJ. High rate of placental infarcts in type 2 compared with type 1 diabetes. J Clin Endocrinol Metab 2012;97:E1160–4.
83. Yetter JF III. Examination of the placenta. Am Fam Physician 1998;57:1045–54.
84. Himes KP, Young A, Koppes E, et al. Loss of inherited genomic imprints in mice leads to severe disruption in placental lipid metabolism. Placenta 2015;36:389–96.
85. Bosquée L, Böttger EC, De Beenhouwer H, et al. Cervical lymphadenitis caused by a fastidious mycobacterium closely related to Mycobacterium genavense in an apparently immunocompetent woman: diagnosis by culture-free microbiological methods. J Clin Microbiol 1995;33:2670–4.
86. Chakravorty S, Sen MK, Tyagi JS. Diagnosis of extrapulmonary tuberculosis by smear, culture, and PCR using universal sample processing technology. J Clin Microbiol 2005;43:4357–62.
87. Benjamin RJ, Wagner SJ. The residual risk of sepsis: modeling the effect of concentration on bacterial detection in two-bottle culture systems and an estimation of false-negative culture rates. Transfusion 2007;47:1381–9.
88. Virolainen A, Salo P, Jero J, Karma P, Eskola J, Leinonen M. Comparison of PCR assay with bacterial culture for detecting Streptococcus pneumoniae in middle ear fluid of children with acute otitis media. J Clin Microbiol 1994;32:2667–70.
89. Rantakokko-Jalava K, Nikkari S, Jalava J, et al. Direct amplification of rRNA genes in diagnosis of bacterial infections. J Clin Microbiol 2000;38:32–9.
90. Carlson CA, Bates NR, Ducklow HW, Hansell DA. Estimation of bacterial respiration and growth efficiency in the Ross Sea, Antarctica. Aquatic Microbial Ecology. AME 19:229-44.
91. Fraser FJ. A selective stain for mitotic figures, particularly in the developing brain. Stain Technol 1982;57:219–24.
92. Stevens JR, Casanova M, Poltorak M, Germain L, Buchan GC. Comparison of immunocytochemical and Holzer's methods for detection of acute and chronic gliosis in human postmortem material. J Neuropsychiatry Clin Neurosci 1992;4:168–73.
93. Marshall JS, Ford GP, Bell EB. Formalin sensitivity and differential staining of mast cells in human dermis. Br J Dermatol 1987;117:29–36.
94. Engbaek K, Johansen KS, Jensen ME. A new technique for Gram staining paraffin-embedded tissue. J Clin Pathol 1979;32:187–90.
95. Brown RC, Hopps HC. Staining of bacteria in tissue sections: a reliable gram stain method. Am J Clin Pathol 1973;60:234–40.
96. Becerra SC, Roy DC, Sanchez CJ, Christy RJ, Burmeister DM. An optimized staining technique for the detection of Gram positive and Gram negative bacteria within tissue. BMC Res Notes 2016;9:216.
97. Bonnekoh B, Wevers A, Jugert F, Merk H, Mahrle G. Colorimetric growth assay for epidermal cell cultures by their crystal violet binding capacity. Arch Dermatol Res 1989;281:487–90.
98. Daya D, Sabet L. The use of cytokeratin as a sensitive and reliable marker for trophoblastic tissue. Am J Clin Pathol 1991;95:137–41.
99. Lai C, Healy E. The Warthin-Starry stain for detection of cutaneous melanin: more than a historical curiosity. Exp Dermatol 2016;25:763–4.
100. Browne HP, Forster SC, Anonye BO, et al. Culturing of 'unculturable' human microbiota reveals novel taxa and extensive sporulation. Nature 2016;533:543–6.
101. Wade W. Unculturable bacteria - The uncharacterized organisms that cause oral infections. J R Soc Med 2002;95:81–3.
102. Brown RC, Hopps HC. Staining of bacteria in tissue sections: a reliable gram stain method. Am J Clin Pathol 1973;60:234–40.
103. DeLong EF, Wickham GS, Pace NR. Phylogenetic stains: ribosomal RNA-based probes for the identification of single cells. Science 1989;243:1360–3.

Author and article information

From the Department of Obstetrics & Gynecology, Division of Maternal-Fetal Medicine (Drs Seferovic, Pace, Carroll, Chu, Racusin, and Aagaard; Mr Belfort), Interdepartmental Program in Translational Biology and Molecular Medicine (Drs Chu, Versalovic, and Aagaard), and Departments of Virology & Microbiology (Dr Versalovic), Molecular & Human Genetics (Drs Versalovic and Aagaard), and Molecular & Cell Biology (Dr Aagaard), Baylor College of Medicine, Houston, Texas; and the Department of Pathology & Immunology, Baylor College of Medicine and Texas Children's Hospital, Houston, Texas (Ms Major and Drs Castro, Muldrew, and Versalovic).

Received Dec. 18, 2016; revised April 6, 2019; accepted April 26, 2019.

The authors report no conflict of interest.

The effort for this work was funded by the March of Dimes Preterm Birth Research Initiative (K.A.), Burroughs Welcome Fund Preterm Birth Initiative (K.A.), and the NIH (1R01NR014792, 6R01DK089201, R01HD091731, NICHD N01-HD-80020 NCS Formative Research all to K.A.).

This work was previously presented at the SMFM Pregnancy Meeting, Atlanta, GA, Feb. 4, 2016; Poster #245.

Corresponding author: Kjersti Aagaard, MD, PhD, FACOG. aagaardt@bcm.edu

Glossary of Terms

ASV: Amplicon sequence variants; sequence variations that denote taxonomic classification based on comparison and matching to a reference database of organisms

Community structure: Used most commonly to refer to the taxonomic composition of and/or the relative abundances of members within a microbial community (eg, microbiome); can also refer to the spatiotemporal distribution of taxa

Diversity: Alpha diversity is a measure of the taxonomic distribution within a community, either in terms of distinct taxa or in terms of their evolutionary/phylogenetic distance, while beta diversity refers to the same metrics measured between communities

Gnotobiotic: A host animal containing a defined set of microorganisms, either synthetically implanted or transferred from another host; often used to refer to model organisms with humanized microbiota

Germ-free gnotobiotic: A host animal containing no microorganisms

Gram stain: Traditional bacterial staining technique that differentiates bacteria into gram-positive and gram-negative groups by detecting peptidoglycan in the cell wall of gram-positive organisms; not all bacteria stain with Gram stain, giving rise to gram-variable and gram-indeterminate groups

Metagenome: The total genomic DNA of all organisms within a community

Metagenomics: The study of uncultured microbial communities, typically relying on high-throughput experimental data and bioinformatic techniques

Microbiome: The total microbial community, genomic content, and biomolecules within a defined environment.

Microbiota: The total collection of microbial organisms within a community, typically used in reference to an animal host

Microflora: An older term used synonymously with microbiota

Warthin—Starry stain: A silver nitrate staining method, which has been historically used to detect poorly staining gram-negative organisms such as spirochetes and small bacilli in complement Gram staining

Whole genome shotgun (WGS) metagenomic sequencing: Used to describe shotgun sequencing of individual organisms and, sometimes, microbial communities; with microbial communities, will be both the host and the microbial genomic content in its entirety

16S rRNA: The transcript of the 16S ribosomal subunit gene, the smaller RNA component of the prokaryotic ribosome, used as the most common taxonomic marker for microbial communities

16S Variable region: One of a series of hypervariable sequence regions within the 16S rRNA, designated 5′ to 3′ as V1—V9 as a basis to distinguish bacterial taxa (eg, V4 as the fourth variable region)

16S rRNA universal ISH probe: In situ hybridization with oligonucleotide probe sets, which hybridize to multiple common shared variable regions in the 16S rRNA gene. By spanning common shared regions, universal probe sets universally detect bacteria in their habitat, such as the placenta villi and microarchitecture, without attempt to speciate taxa.

Appendix

SUPPLEMENTAL TABLE
Predicted functional pathways relative abundance changes

Rank	Pathway	Log(FC)	*P*	FDR	*Q*
1	Ectoine biosynthesis	1.11	<.0001	0.0001	.0000
2	L-histidine degradation II	0.98	<.0001	0.0002	.0000
3	Glucose degradation (oxidative)	1.46	<.0001	0.0004	.0001
4	UDP-2,3-diacetamido-2,3-dideoxy-α-D-mannuronate biosynthesis	1.70	<.0001	0.0005	.0001
5	Ergothioneine biosynthesis I (bacteria)	Und.	<.0001	0.0006	.0005
6	Toluene degradation IV (aerobic) (via catechol)	1.06	<.0001	0.0007	.0007
7	Mevalonate pathway I	0.79	<.0001	0.0008	.0008
8	L-arginine degradation II (AST pathway)	0.94	<.0001	0.0010	.0009
9	Superpathway of geranylgeranyldiphosphate biosynthesis I (via mevalonate)	0.74	<.0001	0.0011	.0016
10	Sucrose degradation II (sucrose synthase)	Und.	.0001	0.0012	.0032
11	Polymyxin resistance	0.95	.0001	0.0013	.0041
12	2-methylcitrate cycle I	0.67	.0001	0.0014	.0038
13	Superpathway of pyrimidine deoxyribonucleoside salvage	0.05	.0001	0.0015	.0036
14	2-methylcitrate cycle II	0.65	.0002	0.0017	.0051
15	Cis-vaccenate biosynthesis	-0.10	.0004	0.0018	.0109
16	Pyrimidine deoxyribonucleotides biosynthesis from CTP	Und.	.0004	0.0019	.0115
17	Pyrimidine deoxyribonucleotides de novo biosynthesis IV	Und.	.0005	0.0020	.0119
18	Nitrate reduction I (denitrification)	0.77	.0005	0.0021	.0117
19	Gondoate biosynthesis (anaerobic)	-0.09	.0006	0.0023	.0139
20	Glycine betaine degradation I	Und.	.0006	0.0024	.0134
21	L-glutamate degradation VIII (to propanoate)	Und.	.0008	0.0025	.0160
22	L-methionine biosynthesis III	-0.06	.0013	0.0026	.0255
23	Isoprene biosynthesis II (engineered)	0.95	.0023	0.0027	.0424
24	Nitrate reduction VI (assimilatory)	-0.45	.0023	0.0029	.0408
25	Methyl ketone biosynthesis	0.85	.0026	0.0030	.0436
26	Peptidoglycan biosynthesis IV (*Enterococcus faecium*)	0.33	.0029	0.0031	.0462
27	Glycogen degradation II (eukaryotic)	1.52	.0032	0.0032	.0501
28	Mono-trans, poly-cis decaprenyl phosphate biosynthesis	0.69	.0033	0.0033	.0497
29	Reductive TCA cycle I	0.27	.0034	0.0035	.0497
30	Creatinine degradation I	Und.	.0036	0.0486	.0485

Predicted functional pathway relative abundances were assessed using PICRISt2 from amplicon sequence variants. The average relative abundance was calculated for all samples and compared against the kit negative controls. Nonparametric *t* test assessed for differences in relative abundance, then *P* values adjusted for multiple comparisons. Of 423 pathways, 30 were enriched or depleted significantly by after Benjamini-Hochberg correction ($Q < .05$).

FDR, false discovery rate; *log(FC)*, log fold change.

Seferovic et al. Visualization of placental microbiota. Am J Obstet Gynecol 2019.